Marine Pollution Bulletin 193 (2023) 115159

Contents lists available at ScienceDirect

Marine Pollution Bulletin

journal homepage: www.elsevier.com/locate/marpolbul

Decadal decline of dominant copepod species in the North Sea is associated with ocean warming: Importance of marine heatwaves

Ilias Semmouri [a,b,*], Karel A.C. De Schamphelaere [a], Jonas Mortelmans [c], Jan Mees [c,d], Jana Asselman [b], Colin R. Janssen [a,b]

[a] Ghent University, Laboratory of Environmental Toxicology and Aquatic Ecology, Faculty of Bioscience Engineering, 9000 Ghent, Belgium
[b] Blue Growth Research Lab, Ghent University, Bluebridge, Wetenschapspark 1, 8400 Ostend, Belgium
[c] Flanders Marine Institute VLIZ, InnovOcean Campus, Jacobsenstraat, 8400 Ostend, Belgium
[d] Ghent University, Marine Biology Research Group, Faculty of Sciences, 9000 Ghent, Belgium

ARTICLE INFO

Keywords:
Zooplankton
Copepoda
Time-series
Belgian part of the North Sea
Climate change
Marine heatwaves

ABSTRACT

Time-series are crucial to understand the status of zooplankton communities and to anticipate changes that might affect the entire food web. Long-term time series allow us to understand impacts of multiple environmental and anthropogenic stressors, such as chemical pollution and ocean warming, on the marine ecosystems. Here, a recent time series (2018–2022) of abundance data of four dominant calanoid and one harpacticoid copepod species from the Belgian Part of the North Sea was combined with previously collected (2009–2010, 2015–2016) datasets for the same study area. The time series reveals a significant decrease (up to two orders of magnitude) in calanoid copepod abundance (*Temora longicornis*, *Acartia clausi*, *Centropages* spp., *Calanus helgolandicus*), while this was not the case for the harpacticoid *Euterpina acutifrons*. We applied generalized additive models to quantify the relative contribution of temperature, nutrients, salinity, primary production, turbidity and pollution (anthropogenic chemicals, i.e., polychlorinated biphenyls and polycyclic aromatic hydrocarbons) to the population dynamics of these species. Temperature, turbidity and chlorophyll *a* concentrations were the only variables consistently showing a relative high contribution in all models predicting the abundances of the selected species. The observed heat waves which occurred during the summer periods of the investigated years coincided with population collapses (versus population densities in non-heatwave years) and are considered the most likely cause for the observed copepod abundance decreases. Moreover, the recorded water temperatures during these heatwaves correspond to the physiological thermal limit of some of the studied species. As far as we know, this is the first study to observe ocean warming and marine heat waves having such a dramatic impact (population collapse) on the dominant zooplankton species in shallow coastal areas.

1. Introduction

Climate change is affecting our oceans and seas, leading to elevations in water temperature and changes to ocean chemistry, sea-level, and oceanographic currents (Stocker et al., 2013). The average temperature of the global ocean surface increased by 0.88 [0.68 to 1.01] °C (90 % confidence interval) over the past 150 years (IPCC, 2021). 0.60 °C of this increase occurred between 1980 and 2020, indicating a recent acceleration of the warming (IPCC, 2021). Recently, the North Sea was observed to warm the fastest in the entire Atlantic for the period 1980–2020, with a warming of the sea surface temperature of 0.39 ± 0.06 °C per decade (1.58 ± 0.25 °C change; Kessler et al., 2022). Moreover, in response to past and current greenhouse gas emissions, future ocean warming will continue to be perpetuated for the coming centuries (Cheng et al., 2019; IPCC, 2021). For example, the IPCC projects that under representative concentration pathway (RCP) 8.5 in the period 2017–2100, the ocean heat content in the upper 2000 m of the water column will increase ~5–7 times as compared to the 1970 to 2017 period (IPCC, 2019). Lately, the increase in the occurrence of extreme events associated with global climate change, such as summer heat waves, has attracted more attention from research in both regional and global earth systems (IPCC, 2021). Consequently, these heatwave events

* Corresponding author at: Ghent University, Laboratory of Environmental Toxicology and Aquatic Ecology, Campus Coupure, Building F – 2nd Floor, Coupure Links 653, B-9000 Ghent, Belgium.
E-mail address: ilias.semmouri@ugent.be (I. Semmouri).

https://doi.org/10.1016/j.marpolbul.2023.115159
Received 4 February 2023; Received in revised form 31 May 2023; Accepted 6 June 2023
Available online 15 June 2023

cause anomalously warm seawater in relatively short time periods via local air-sea heat flux exchanges, which are also known as marine heatwaves (MHWs) (Chen et al., 2022; Hobday et al., 2016). Nearly 70 % of global oceans experienced strong or severe heatwaves in 2016, an increase from 30 % compared to data from 2012 (Hobday et al., 2018). So far, few studies have examined the impact of these MHW on marine biodiversity, but documentation of disturbance by these MHW events to marine ecosystems and their services is increasing (Smale et al., 2019).

Marine ecosystems provide important ecosystem services on which man depends (Townsend et al., 2018). While fish and associated fisheries provide are well known (Holmlund and Hammer, 1999), other marine key organisms – which are often overlooked and understudied – also contribute to these services. The mesozooplankton, for example, comprise an important connection between phytoplankton and higher trophic levels (e.g., several (often commercial) pelagic fish and some marine birds and mammals). It further contribute to the carbon cycle (and the benthic zone) through formation of marine snow, the sedimentation of dead carcasses and faecal pellets (Wexels Riser et al., 2002). Hence, zooplankton supply to the role of pelagic ecosystems as carbon dioxide sources or sinks and other greenhouse gasses as well, throughout the generation of detritus, i.e., marine snow (Kiørboe, 2001). Hence, zooplankton responses to changes in environmental variables are likely to induce elemental changes in the established dynamics of marine ecosystems, causing fluctuations in primary production and other environmental conditions that ultimately will translate into the higher trophic levels (Buttay et al., 2015). Environmental variability is rapidly reflected in zooplankton population dynamics due to their typically short life cycles (Bellier et al., 2022; Hays et al., 2005). These organisms have consequently been suggested as sentinel species for climate change and ocean warming in particular (Buttay et al., 2015; Hays et al., 2005). Plankton are recognised to provide important knowledge on the state of pelagic ecosystems, their dynamics, and the functioning of the marine food web (e.g., O'Brien et al., 2011; Castellani and Edwards, 2017). Although monitoring of zooplankton assemblages (such as the Continuous Plankton Recorder, CPR) has been conducted in the marine environment around the world since the early 20th century (e.g., Batten et al., 2003; O'Brien et al., 2017), spatiotemporal variations in the composition of zooplankton assemblages and plankton dynamics in general remain poorly known, even in well-studies areas like the North Sea.

The southern Bight of the North Sea, including the Belgian Part of the North Sea (BPNS, Fig. 1), is a shallow, well-mixed basin, characterised by subtidal sandbanks that run parallel to the coast. The BPNS is a eutrophic ecosystem as a result of nutrient inputs via the discharge of the prominent western European rivers Rhine, Meuse and Scheldt (Lacroix et al., 2004; Daro et al., 2006). The area is heavily influenced by anthropogenically induced impacts such as dredging and shipping (access to the ports of the Hamburg-Le Havre range) incl. The import of invasive and potentially harmful species, aggregate extraction, anchorage zones, historical dumping sites, professional bottom trawling, recreational fisheries, the construction of offshore wind farms and other infrastructure engineering, and pollution (Lescrauwaet et al., 2013). Recent mesoscale zooplankton surveys in the BPNS – documenting species composition and seasonal zooplankton dynamics – have been carried out by Van Ginderdeuren et al. (2014), Deschutter et al. (2017), Semmouri et al. (2020a, 2020b, 2021) and the LifeWatch observatory (Flanders Marine Institute, 2021, 2021b; Mortelmans et al., 2019, 2021; Ollevier et al., 2021). The zooplankton community is dominated by copepods, the key group in terms of abundance and biomass. Their biomass usually surpasses 80 % of the total zooplankton biomass (Williams et al., 1994). Mortelmans et al. (2021) observed that harpacticoid and calanoid copepods combined constitute 70.15 % of the total zooplankton abundance in the BPNS. The copepod species assemblages in the BPNS are mainly represented by four taxa in terms of abundance:

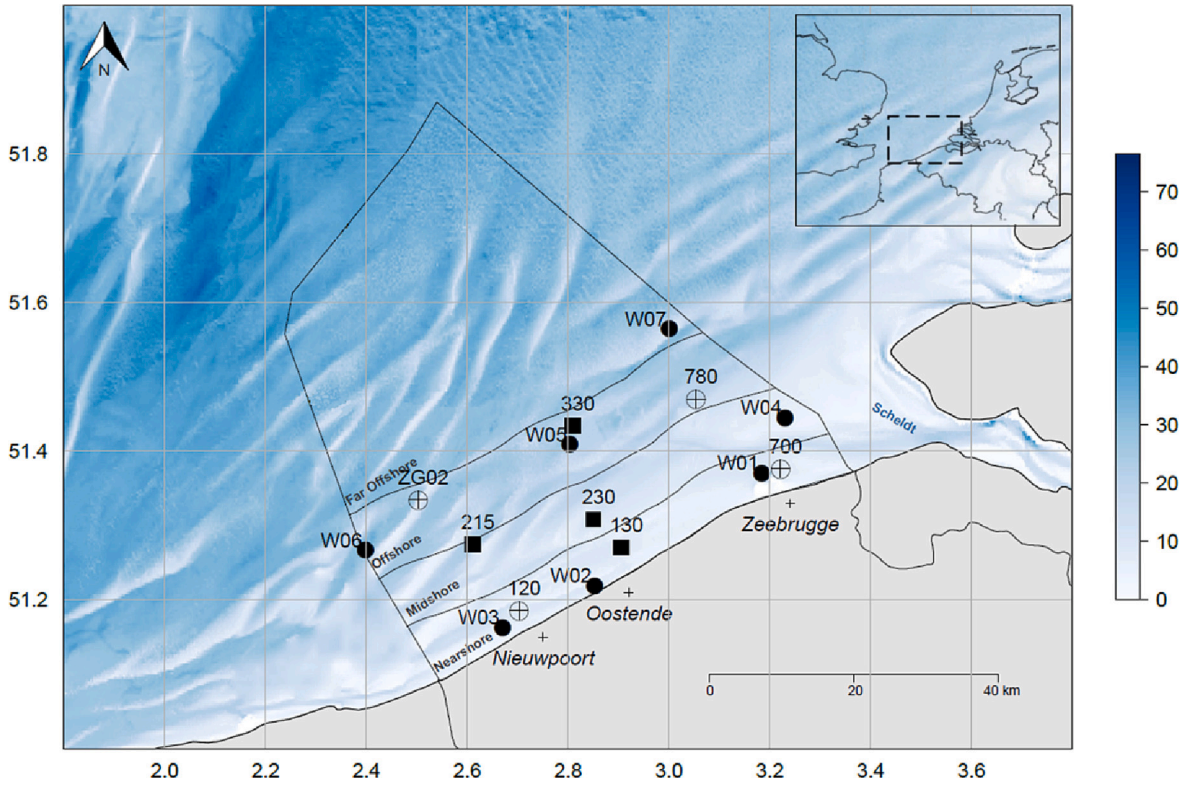

Fig. 1. Map showing sampling locations and names of sampling stations in the Belgian Part of the North Sea (BPNS) of this study (squares) and stations sampled by Van Ginderdeuren et al. (2014, closed circles) and Deschutter et al. (2017, open circles). Please note that stations 130 and 330 have been sampled in both this study and by Deschutter et al. (2017). The nearshore, midshore, offshore and far offshore zones are indicated on the map. The crosses indicate the location of three coastal cities. Bathymetry reported in meter (m). Modified from Mortelmans et al. (2019) with authorisation from the authors.

the calanoids *Acartia clausi* (Giesbrecht, 1889), *Temora longicornis* (Müller, 1785), *Centropages* spp. (Krøyer, 1849) and the harpacticoid *Euterpina acutifrons* (Dana, 1847) (Deschutter et al., 2017; Semmouri et al., 2021; Van Ginderdeuren et al., 2014).

To comprehend population dynamics in the context of higher climatic variability and increasing anthropogenic pressure, long-running datasets from ocean observation programs are crucial to understand and to improve predictions about potential changes that might affect the functioning of marine ecosystems and the services they provide. As discussed profoundly in Mortelmans et al. (2021), such data from the Belgian Part of the North Sea (BPNS) is scarce. A notable exception is recent work of the same authors (Mortelmans et al., 2021), who used the ZooScan plankton imaging device (Gorsky and Grosjean, 2003; Grosjean et al., 2004), enabling a rapid and automated assessment of abundance, size and biomass estimations of preserved plankton samples to investigate copepod population dynamics. However, the taxonomic resolution of their dataset is rather low, as it provides counts on the level of orders (i.e., calanoid, harpacticoid copepods), hence, missing important changes at the species level (as described in Mortelmans et al., 2021). Yet, information at the species level is crucial, as certain species contribute more extensively to the food web than other species. For example, Van Ginderdeuren et al. (2013) reported that the common calanoid copepod species *A. clausi*, is barely preyed upon by the pelagic fish stocks in the BPNS, in contrast to the calanoid *T. longicornis*, which is one of the main prey items of sprat, herring and mackerel. Therefore, in the current study we examined the links between copepod dynamics (at the species level) and changes in environmental factors by analysing a long-term zooplankton time series. This time series was established by pooling data from two published studies and that of a newly generated dataset in the BPNS, in total covering information of 14 years (2009–2022). The aim of this study is to delineate the seasonal and interannual variations in the abundances of five copepod species in the BPNS and to study the importance of the main environmental factors to explain the copepod density changes, with a focus on the effects of temperature and chemical pollution.

2. Material & methods

2.1. Sampling

Zooplankton were sampled with the research vessel (RV) Simon Stevin during 44 different sampling campaigns performed from 2018 through 2022 (start: 20th February 2018, end: 12th of December 2022) at four different stations in the BPNS (Fig. 1). In 2018 and 2019, samples were taken in bimonthly sampling campaigns. Due to the COVID-19 pandemic and the associated restrictions in spring 2020, the sampling strategy for 2020 till 2022 was adapted to collecting samples monthly, due to uncertainty of the situation and the prevailing regulations. Two nearshore and two offshore stations were chosen: the nearshore stations were stations 130 and 230, situated approximately four and ten km off the harbour of Ostend, Belgium, respectively (Fig. 1). The two offshore stations were station 215, situated on the Flemish banks in the western part of the BPNS, and the more eastern station 330, located approximately 17 and 24 km from the coast, respectively (Fig. 1). Sampling time and GPS locations are provided in Supplementary Table 1. In total, 170 zooplankton samples (86 nearshore, 84 offshore) were collected. The sampling was conducted simultaneously to the long-running sampling and monitoring efforts by Flanders Marine Institute (VLIZ), Belgium (2021, 2021b).

Zooplankton was sampled using a vertically towed WP2 net (57 cm diameter, 200 μm mesh size), fitted with a flow meter that was towed in an oblique haul from bottom to surface. The zooplankton samples were fixed and stored in a 70 % ethanol solution and were subsequently used for species identification. In the lab, the copepodite stages of the calanoid copepods *Temora longicornis, Acartia clausi, Centropages* spp., *Calanus helgolandicus* (Crustacea, Copepoda, Calanoida) and the pelagic harpacticoid copepod *Euterpina acutifrons* (Crustacea, Copepoda, Harpacticoida) were identified and counted using a stereomicroscope (Leica MZ 10). The species *Centropages hamatus* and *Centropages typicus* densities were pooled due to uncertainties identifying the copepodite stages of both species.

2.2. Measurements of environmental variables

At each sampling station, conductivity (μS/cm), temperature (°C) and depth (m) profiles were collected with a Seabird SBE25plus CTD (Flanders Marine Institute (VLIZ), Belgium, 2021). Additionally the following parameters were quantified at 3 m depth: salinity of the water body (−), the density of the water body (kg/m^3), the pressure of the water body (decibel; CTD derived), the sound velocity through the water body (m/s), the optical backscatter (OBS) as turbidity of the water body, expressed in Nephelometric Turbidity Units (NTU), the concentration of Suspended Particulate Matter (SPM) in the water body (expressed in mg/L) and the Secchi Depth (cm) as a proxy for the transparency the water body.

Water samples, collected at a depth of 3 m, were taken with Teflon-coated Niskin bottles and were subsequently analysed for nutrient and pigment concentrations by the LifeWatch observatory as part of the Flemish contribution to the LifeWatch ESFRI by the Flanders Marine Institute (Flanders Marine Institute (VLIZ), Belgium, 2021b). Each time, 200 mL of seawater was filtered with a cellulose-acetate filter (pore size 8.0 μm, ⌀ 47 mm, Cytiva) for nutrient analyses. Nutrients were analysed using a QuAAtro39 Continuous Segmented Flow Analyzer (SEAL Analytical GmbH, Norderstedt, Germany): water samples and reagents were continuously pumped through a heated chemistry manifold (37 °C), resulting in a specific colour of which the intensity is proportional to the concentration of the specific nutrient. The following nutrients were measured: nitrate (NO_3^-), nitrite (NO_2^-), phosphate (PO_4^{3-}) and silicate (SiO_4^{4-}) concentrations.

In regard to the pigment analyses, a vacuum pump and corresponding filter unit, in combination with Whatman GF/F glass fibre filters (47 mm) was applied to filter as much seawater as possible to saturate the filter (Mortelmans et al., 2019). After the filter ran dry, the sides of the sample container were flushed clean thoroughly with Milli-Q water. The filter was stored in a 2 mL storage unit in liquid nitrogen. High Pressure Liquid Chromatography (HPLC) was subsequently used to determine the identity and quantity of the pigments, according to the protocols described in Mortelmans et al. (2019).

The concentrations of polychlorinated biphenyls (PCB) and polycyclic aromatic hydrocarbons (PAH) in the seawater, used as proxies for anthropogenic pollution, were determined at each sampling location, in samples of 5 L seawater, of which 4 L were retained per sample for the analyses. The concentration of these compounds was quantified with gas chromatography–mass spectrometry after liquid extraction of the filtered (0.7 μm) water samples. To do so, internal standards (deuterated analogues of parent PAH compounds (Dr. Ehrenstorfer, VWR) and PCB congeners 14, 112, 143, 155 and 204 (Supelco/Dr. Ehrenstorfer, Sigma-Aldrich/VWR)) were added to the 4 L volumes of water, which were extracted three times with dichloromethane. The extract was subsequently dried on Na_2SO_4 and concentrated to about 5 mL using a rotary evaporator, followed by concentration under N_2 to 0.2 ml. Anthracene-d_{10} (Dr. Ehrenstorfer, VWR) was added as recovery standard. The extracts were concentrated and analysed with a gas chromatography–mass spectrometer (GC–MS, Thermoquest, Austin, Texas, USA). The extracts were injected (1 μL) on a 30 m * 0.25 mm DB5-ms cross-linked fused silica capillary (0.25 μm film thickness). The carrier gas was helium (99.999 %) at a linear flow of 1 mL min^{-1}. Splitless injection at an injection temperature of 230 °C was performed. Column initial temperature was kept at 55 °C during injection and its temperature increased at 15 °C min^{-1} to 310 °C which was held for 6 min. Via a transfer line heated to 310 °C, the GC column was directly coupled to the ion source of the MS mass spectrometer. The quadruple MS operated in

the selected ion monitoring electron ionization mode with the ion source at 250 °C. All solvents used were of purity suitable for organic residue analysis.

As in Deschutter et al. (2017), PAH and PCB concentrations were multiplied with their corresponding octanol/water partition coefficient (K_{ow}) and subsequently converted to molar concentrations, before summation (sum_PCBs, sum_PAHs):

$$\mathrm{sum_{PCBs}}, \mathrm{sum_{PAHs}} = \sum_i \left(\left(concentration_i * K_{ow,i} \right) \Big/ M_i \right) \quad (1)$$

With concentration being the concentration of the PAH/PCB compound i (μg/L), and M representing its molecular weight, expressed in g. mol^{-1}. The octanol/water partition coefficient (K_{ow}), a measure of a compound's hydrophilicity/lipophilicity, is defined as the equilibrium ratio of the chemical's concentrations in octanol over water at a certain temperature (Cumming and Rücker, 2017). It is an important characteristic of a substance as it influences to a large extent the compound's fate both in the environment as well inside a living organism (Cumming and Rücker, 2017). Compounds with a high K_{ow} are more inclined to adsorb more easily to organic matter and accumulate more readily in lipid tissue because of their lower affinity for water and thus higher affinity for lipid-rich matrices (Chiou, 1985; ECHA, 2008). Similar as in Deschutter et al. (2017), PCB and PAH concentrations were therefore summed after multiplication with their K_{ow} values (Eq. 1), assuming nonpolar narcosis to be the major mode of action for both categories of toxicants (McCarty and Mackay, 1993). Toxicant concentrations are thus expressed as μmol POPs /kg lipid weight.

2.3. Continuous temperature measurements at Thornton bank

Additionally, temperature data (air temperature (°C) and seawater temperature at approximately 1.1 m depth (°C)) was collected every hour for the period 2018–2022 from an offshore buoy situated at sampling station W07 at the Thornton bank (51.58 Lat. 2.993 Long.), approximately at 30 km off the Belgian coast (Zeebrugge) (Flanders Marine Institute, 2022).

2.4. Data series and data integration

Zooplankton abundance and environmental data in this study is derived from three different datasets: (1) data obtained from the current study (2018–2022, see Sections 2.1 and 2.2), (2) a dataset previously generated by our laboratory in 2015 and published by Deschutter et al. (2017) and (3) a zooplankton dataset collected by Van Ginderdeuren et al. (2014) between 2009 and 2010. The datasets cover 4, 6, and 7 stations in the BPNS, respectively (Fig. 1). Nearshore station 130 and offshore station 330 have been sampled in both this study and in the study of Deschutter et al. (2017). The far offshore samples collected by Van Ginderdeuren et al. (2014) were not included in this study, as the zooplankton community is relatively different and no comparable sampling stations in proximity were visited in the recent sampling campaigns. Both Deschutter et al. (2017) and Van Ginderdeuren et al. (2014) used the same sampling protocol as used in this study, hence, yielding a comparable time series. In total, data are derived from 376 different samples.

2.5. Statistics

All statistical tests were executed in R Studio. Prior to all analyses, outliers were detected by means of Cleveland dotplots and withdrawn from further analyses. The Shapiro-Wilk test of normality and Levene's test of homogeneity of variances were applied as pre-tests to all data. Differences between densities collected at different years, seasons or locations were statistically analysed using the non-parametric Kruskal-Wallis test, followed by a pairwise Wilcoxon test. Differences were considered statistically significant if the Benjamini-Hochberg (BH) adjusted *p*-value was smaller than 0.05. Spearman rank correlation analyses were applied to determine the correlations among the environmental variables and copepod abundances.

The seasonal variability as well the spatial distribution in the copepod community composition (i.e., the 5 investigated species) was visualised using a Principal Component analysis (PCA) and a corresponding correlation circle, after log-transformation of the abundance data using the Factoextra, FactoMineR v.2.0, corrplot and ggplot packages in R v.4.1.1. In the correlation circle, each recorded species is represented as a vector, which signals the combined strength of the relationships between the taxon and the two PCs (i.e., the vector length) and whether these associations are positive or negative (i.e., the vector direction). The angle between two vectors signals the degree of correlation between two taxa (0° = indicates a complete positive correlation, an adjacent angle indicates a highly positive correlation, an orthogonal angle (90°) indicates that the two variables are completely uncorrelated, and opposite angles (180°) indicate a completely negative correlation).

The Bray–Curtis distance on log transformed abundance data was used to estimate the degree of dissimilarity between the samples. To test the hypothesis that copepod communities differ in time and/or space, the Bray–Curtis dissimilarity matrices were ordinated by Multidimensional Scaling (MDS) and the stress level, or measure of the goodness of fit, was computed for the ordination. We tested the difference between community states by applying a Permutational Multivariate Analysis of Variance (PERMANOVA) with 999 permutations (Anderson, 2001), implemented by the 'adonis' function in the vegan package v.2.5.2 (Oksanen et al., 2015). Here, a Bray–Curtis dissimilarity matrix, calculated from log transformed copepod abundance data, was used to be representative of the community composition. Timing of sampling (both month and year), as well as sampling location, were used as predictor variables.

2.6. GAM modelling and covariate selection

Generalized additive models (GAMs) were applied to identify and quantify the main drivers of the abundance of four of the five investigated copepod taxa in the BPNS. Densities of *C. helgolandicus* were not suited for this kind of models as this species was mostly absent in our samples (Fig. 2), causing a considerable discrepancy among the estimates of the basic functions composing the smoothers for this taxon. In contrast to generalized linear models, who are restricted to the assumption that all explanatory variables are linked in a linear combination with the response variable, GAMs can handle nonlinear, non-monotonic relationships between the assortment of explanatory variables and the response variable by applying nonparametric smooth functions of the explanatory variables (Zuur et al., 2009). GAMs were fitted using the "mgcv" package v. 1.8.36 (Wood and Wood, 2016) in R v4.1.1. For each particular model, we modelled the log10 (abundance. m^{-3} + 1) as a function of the environmental predictors. In the current study, the general form of the GAM is proposed by the following equation:

$$E[y] = a + s(V_i) + \cdots + s(V_n) + \varepsilon \quad (2)$$

with E[y] representing the response (dependent) variable y, a representing the intercept of the parametric term that represents the mean of the response variable, s representing the smoothing function based on the thin plate regression spline, V_i representing the independent variables, and ε constitutes the error term.

To assess which parameters would be selected for constructing the GAMs, we first investigated the correlation between the variables (Spearman). To avoid collinearity, variables with a concurvity >0.7 were removed from the analyses after evaluation of their possible ecological significance in the model. Concurvity refers to the generalization of collinearity, referring to the situation where a smooth term

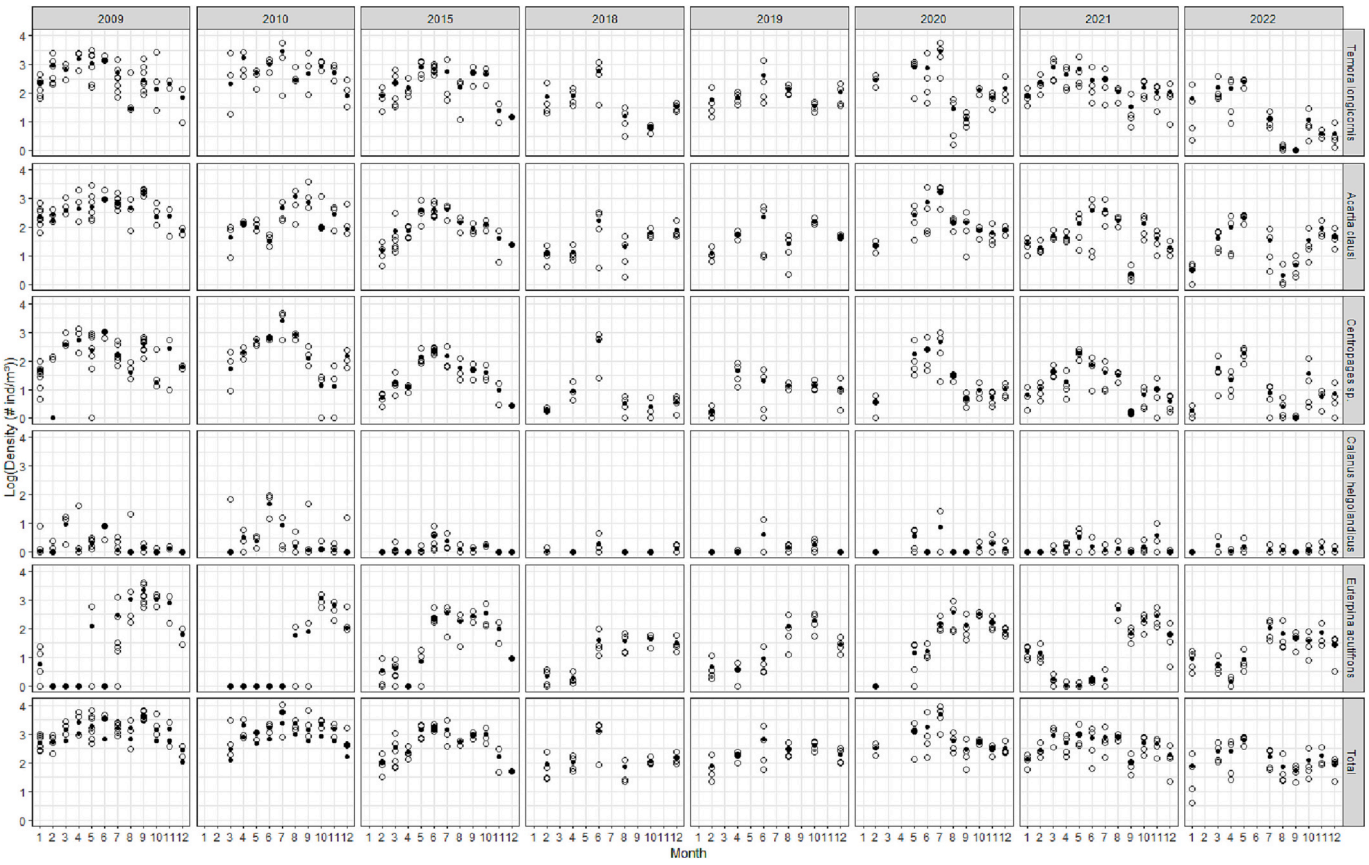

Fig. 2. Log transformed abundances for the calanoid copepods *Temora longicornis*, *Acartia clausi*, *Centropages* spp., and *Calanus helgolandicus*, the harpacticoid *Euterpina acutifrons* and total copepod abundances (bottom row), expressed in ind/m^3, for the periods 2009–2010, 2015 and 2018–2022 in the Belgian Part of the North Sea (white circles). All available samples were included. Mean monthly values are represented by a black dot. Data gaps of four and two years are present between the two periods.

can be estimated by a combination of the other smooths. So far, no universal criteria for concurvity have been defined, but one study discussing the effects of concurvity proposes that values higher than 0.5 start to introduce noticeable errors (He, 2004). The parameters that were selected to construct the GAMs include water temperature, salinity, Secchi depth, chlorophyll *a* concentrations, and the sum of PCB and PAH concentrations.

All GAMs were based on a Gaussian error distribution with smoothing parameters estimated by restricted maximum likelihood (REML) maximization, as described in Wood (2010). Models containing all potential combinations of the selected variables were assembled and were then ranked following Akaike's information criterion (AIC) (Cavanaugh and Neath, 2019). In other words, variables were selected to minimize the AIC and maximize the Spearman rank correlation coefficient. Based on the AIC, the Akaike weight (w_i) of each model, a value between 0 and 1, was calculated as the probability of each model being the best model, given the data and the set of candidate models (e.g., Burnham and Anderson, 2003):

$$w_i = \frac{exp\left(-\frac{1}{2}\Delta_i\right)}{\sum_{x=1}^{X} exp\left(-\frac{1}{2}\ \Delta_x\right)} \quad (3)$$

where Δ_i is equal to the AIC of the best model – AIC of the model of interest i, Δ_x is the AIC of the best model - the AIC of model x, and where the denominator is the sum of Δ_x of all X models that have been tested (Symonds and Moussalli, 2011). The strength of evidence in favour of one model over the other is acquired by dividing their Akaike weights. Therefore, the evidence ratio (ER = $w_{i,b}/w_{i,m}$) was determined to examine whether the model with the highest w_i ($w_{i,b}$) was truly a better model relative to the models with a lower wi ($w_{i,m}$) (Burnham and Anderson, 2003; Symonds and Moussalli, 2011). Any model with an ER $>$ 2 was considered as negligible with respect to the best model (cf. Symonds and Moussalli, 2011).

The residuals of the best fitted model were subsequently used to test for underlying assumptions of normality and homogeneity (Zuur et al., 2009). Homogeneity was concluded, when the variability of the residuals was similar across the range of fitted values. Graphical diagnostics were used to evaluate normality. Normality was assumed if the QQplot displayed a straight line of residuals and when the histogram of the residuals displayed a bell-shaped curve (Wood, 2006; Zuur et al., 2009). The explained deviance was utilised to estimate how much of the variability in the data was explained by the selected models (Zuur et al., 2009). Variables occurring in the best models (ER $\leq$2) were chosen as they contribute in explaining the variability of the dependent variable. The proportion of variance explained by a variable was quantified by calculating the reduction in deviance after fitting an alternative model without the variable respectively.

3. Results

3.1. Trends in population densities

T. longicornis was the most commonly found species, occurring in almost all samples (98 %), followed by *A. clausi* (present in 98 % of the samples), *Centropages* spp. (93 %), *E. acutifrons* (91 %) and *C. helgolandicus* (35 %) (Table S1). *T. longicornis* and *Acartia clausi* can be regarded as wide spread, abundant species in the BPNS all year round and occurring at all stations, reaching high densities (up to 7616 ind.

m^{-3} in July 2010 at station W01 and up to 3735 ind. m^{-3} in September 2010 at station W07, respectively). *Centropages* spp. abundances displayed a similar pattern with densities found up to 4498 ind m^{-3} in July 2010 at station W01. Densities of *C. helgolandicus* remained very low throughout the years with maximum abundances of 96.8 ind m^{-3} (June 2010 at station W07). *E. acutifrons* densities typically peaked from August to December with densities found up to 4250 ind m^{-3} in September 2009 at station W04. Total copepod densities reached a maximum in late spring and early summer, with a second smaller peak in late summer/early autumn in some years (Fig. 2, S1). *T. longicornis* and *A. clausi* both contributed most to the spring peak of copepod abundance, while the autumn peak was associated with increased densities of *T. longicornis* and *E. acutifrons*. There were no significant differences in the densities of *E. acutifrons* between the sampled stations, regardless of time (Kruskal-Wallis, $p > 0.05$), while densities of the calanoid species collected in two nearshore stations (120,130) were

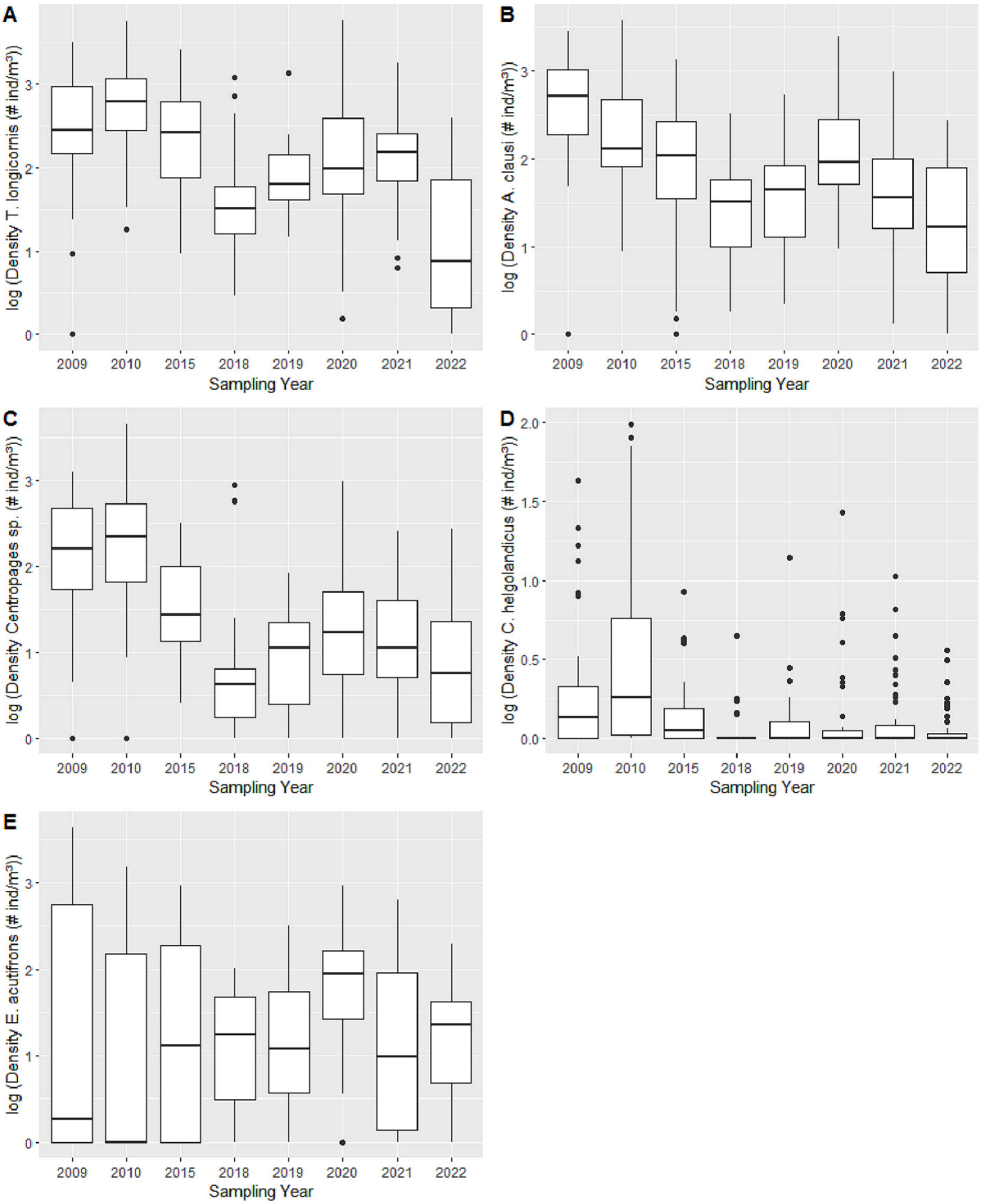

Fig. 3. Boxplot of the log transformed abundances of the copepods *Temora longicornis* (A), *Acartia clausi* (B), *Centropages* spp. (C), *Calanus helgolandicus* (D), and *Euterpina acutifrons* (E) in the BPNS in the last 10 years. The thick black horizontal line represents the median, the box constitutes the upper and lower (25 % and 75 %) quartiles, while the bars represent the data range.

significantly lower compared to the other stations (Pairwise Wilcox test, BH adjusted $p < 0.05$).

Average recorded copepod densities are reported in Table S4. A Kruskal-Wallis test showed that there is a statistically significant difference in average *T. longicornis* densities between the years ($\chi^2(7) = 101.1$, $p < 0.01$), with densities from years 2015 and 2018–2022 being significantly lower compared to the period 2009–2010 (Pairwise Wilcox test, BH adjusted $p < 0.05$; Fig. 3). In 2018 and 2022, *T. longicornis* densities were significantly lower than in any other sampling year. Densities in 2021 were significantly higher than in 2018 and 2019, but not significantly different from 2020 (BH adjusted $p < 0.05$; Fig. 3). The average density of *T. longicornis* in the BPNS in 2020 was 39.4 % lower compared to the average annual from 2010 (Table S4). Except for the densities of the harpacticoid copepod *E. acutifrons* (Kruskal-Wallis, $p > 0.05$), the densities of the other investigated copepod species were significantly different over the sampling years as well (Kruskal Wallis $\chi^2(7)$ of 99.7, 94.9 and 38.4 for *A. clausi*, *Centropages* spp. and *C. helgolandicus*, respectively; $p < 0.01$). *A. clausi* and *Centropages* spp. densities were significantly higher in 2009 and 2010 compared to more recent sampling years (Pairwise Wilcox test, BH adjusted $p < 0.05$; Fig. 3). There is no significant difference in abundance in the years 2019–2022 for *Centropages* spp., while *A. clausi* densities were significantly higher in 2020 ($p < 0.05$; Fig. 3). The average densities of *A. clausi* and *Centropages* spp. in the BPNS in 2020 were 14.1 and 79.8 % lower, respectively, compared to the average annual from 2010 (Table S4). *C. helgolandicus* densities in the period 2015–2021 were significantly lower compared to 2009, but there were no significant density increases or decreases in 2015–2022 (Fig. 3).

3.2. Copepod community analyses

First, the seasonal variability and spatial distribution in the copepod community composition was visualised using a PCA analysis. 50.2 % and 21.6 % of the variance is explained by the first and second axis of the PCA analysis, respectively (Fig. 4). The first axis is most strongly correlated to calanoid densities, while the second axis mainly is associated with *E. acutifrons* densities (Fig. 4). *T. longicornis* densities were significantly correlated with *Centropages* spp., *A. clausi* and *C. helgolandicus* densities (Spearman Rho of 0.61, 0.65 and 0.42, respectively, $p < 0.01$), but not with *E. acutifrons* densities ($p > 0.05$). Only, *A. clausi* abundances correlated significantly with *E. acutifrons* abundances (Spearman Rho of 0.21, p value <0.01). The copepod densities clearly show clustering according to sampling time (sampling season, i.e., month), while this was not the case for sampling location or year (Fig. 4).

To enhance our understanding of changes in the structure of the copepod community over time/per location, we applied Multidimensional Scaling (MDS) to the calculated Bray–Curtis dissimilarity matrix, as a measure of Beta-diversity. The Nonmetric MDS ordination designated a certain level of separation in the plankton samples, predominantly based on differences in sampling month (Stress = 0.131; Fig. 5). The subsequent PERMANOVA analysis indicated as well that the copepod community composition of the samples differs significantly over time (sampling month: $R^2 = 0.362$, p-value = 0.001; sampling year: $R^2 = 0.160$, p-value = 0.001), as well as over space (p-value = 0.001; Table 1).

3.3. Correlation between copepod densities and environmental variables

Tables S1 and S2 provide an overview of the recorded copepod abundances and the measured environmental parameters per sampled location for every sampling campaign. As expected, we detected seasonal variation in the environmental parameters (Table S2; Fig. S2). Water temperatures, sampled simultaneously with the zooplankton samples (measured at 3 m depth), ranged between 2.8 and 22.5 °C (Table S2), with the lowest temperatures recorded in February and the highest in August. Water temperatures, recorded during the same sampling campaign, were comparable among the stations, but tended to be more extreme in the nearshore stations (yet not significant; $p > 0.05$; Fig. S2, S3). Irrespective of seasonality, there was no significant temperature difference in the sea water over the years (Kruskal Wallis, $p > 0.05$). However, water temperatures were significantly higher in the summer months of 2022 compared to previous summer periods (Fig. 6). Similarly, the winter period of 2020 was significantly warmer than the winter months from the other studied years, except for 2019 (pairwise Wilcoxon test, $p < 0.05$; Fig. 6). All copepod species correlated positively with sea water temperatures (Spearman Rho; $p < 0.05$), but this correlation was most profound in *A. clausi* and *Centropages* (Fig. 7). However, when investigating these correlations for each sampling season, we found a negative correlation (Spearman Rho, $p < 0.01$) between calanoid densities and water temperatures (Fig. 6, S4).

During the five years of sampling (2018–2022), Belgium experienced seven different heat waves, resulting in remarkably higher seawater temperatures, as measured continuously by the buoy situated at the Thornton Bank since 2016 (Fig. S5, Table 2). The Royal Meteorological Institute of Belgium (RMI) defines a national heatwave as a period of at least 5 consecutive days when the maximum temperature measured at their institute in Brussels (Uccle) reaches at least 25 °C and > 30 °C for minimum three days (RMI, 2022). These increases in water temperature coincided with sharp decreases in calanoid copepod abundances (Fig. 6, S4).

Chlorophyll *a* concentrations typically peaked in March and April, and generally reduced along a nearshore – offshore gradient (Table S2). Regardless of time, we did not find a significant spatial difference in chlorophyll *a* concentrations (Fig. S3). We did not find a significant correlation between chlorophyll *a* concentrations and copepod abundances, regardless of time (Spearman Rho, $p > 0.05$; Fig. 7). However, only considering the spring season, we found a negative correlation between chlorophyll *a* concentrations and *T. longicornis*, *A. clausi* and *Centropages* spp. abundances (Spearman Rho of −0.46, −0.28 and −0.36, respectively; $p < 0.05$). This negative correlation was also found in the summer months for *T. longicornis* (Spearman Rho of −0.3; $p < 0.05$). *A. clausi* and *Centropages* spp. densities exhibited a significant positive correlation with Beta carotene concentrations, regardless of time (Fig. 7).

In terms of nutrient concentrations, nitrates represent the most abundant nutrient with concentrations ranging between 0.06 and 57.33 μmol/L (Fig. S2, Table S2). Calanoid copepod densities correlated negatively ($p < 0.05$) with all measured nutrient concentrations, while for the harpacticoid *E. acutifrons* this was only the case for nitrate concentrations (Fig. 7).

Turbidity was significantly different among the sampling stations, with seawater being significantly more clear in the offshore stations 215 and 330 (Pairwise Wilcox test, BH adjusted $p < 0.05$; Fig. S3). Calanoid copepod densities correlated positively with Secchi depth (more clear sea water; Fig. 7), while was not the case for *E. acutifrons*.

In terms of pollutants, the quantified PAH concentrations kept below the Environmental Quality Standards (EQS) of the Water Framework Directive (WFD; 2000/60/EC) set by the European commission (EC, 2008) and the Flemish government (Vlaamse regering, 2010) (Table S2, S3), while the measured PCB concentrations regularly surpassed these norms (Table S2, S3). We did not find a significant correlation between summed PCB or PAH concentrations and copepod abundances in our dataset ($p > 0.05$).

3.4. Models on copepod species abundances

For each species one model was selected based on the AIC (Table 3; Fig. S6-S9). The models had an overall fit explaining between 45.8 % (*T. longicornis*) and 59.6 % (*Centropages* spp.) of the variability (Table 3). Temperature, Secchi depth and chlorophyll concentrations are the only environmental variables incorporated in the GAM models for all

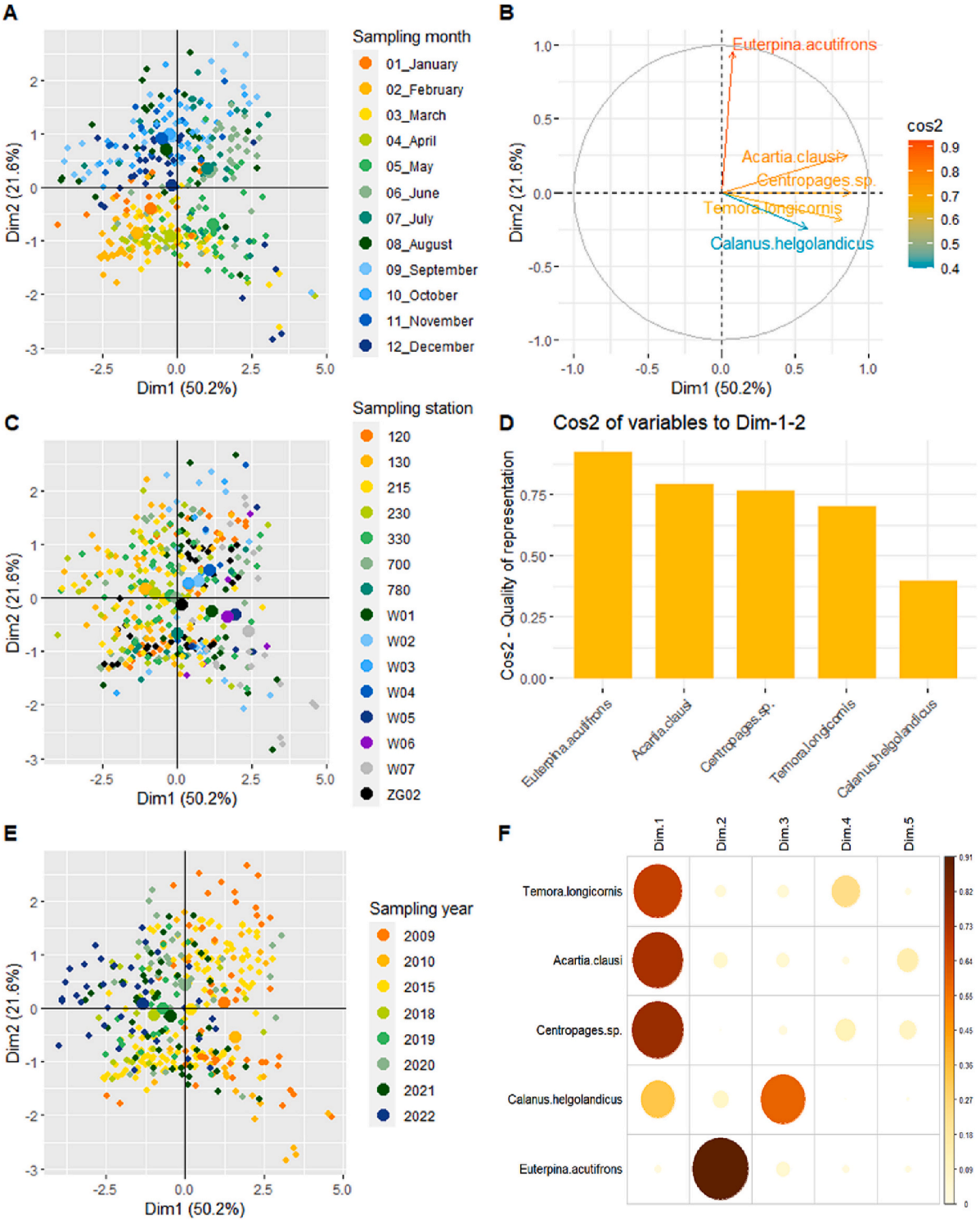

Fig. 4. Principal component analyses (PCA) and correlation circle plot generated for the log transformed copepod densities for every sample in the 2009–2022 period. (A,C,E) PCA plots focusing on clustering patterns for sampling month, station or sampling year. Single points refer to an individual plankton sample taken at a specific time (month, year) and sampling station, as indicated in the legend. (B) correlation circle plot. Vectors are the loadings on PC1 (x-axis) and PC2 (y-axis). The quality of representation of the variables (taxa) is indicated by the squared cosine (cos2). A high cos2 value indicates a good representation of the taxon on the principal component. Vector length indicates the strength of the relationship and the angle between two vectors gives the degree of correlation (adjacent = highly correlated taxa, orthogonal (90°) = uncorrelated taxa, and opposite (180°) = negatively correlated taxa). (D) Bar plot of variables cos2 for the first two principal components, as indicator of representation of the variable by the two principal components. (F) Correlation plot of the cos2 of variables on all the dimensions.

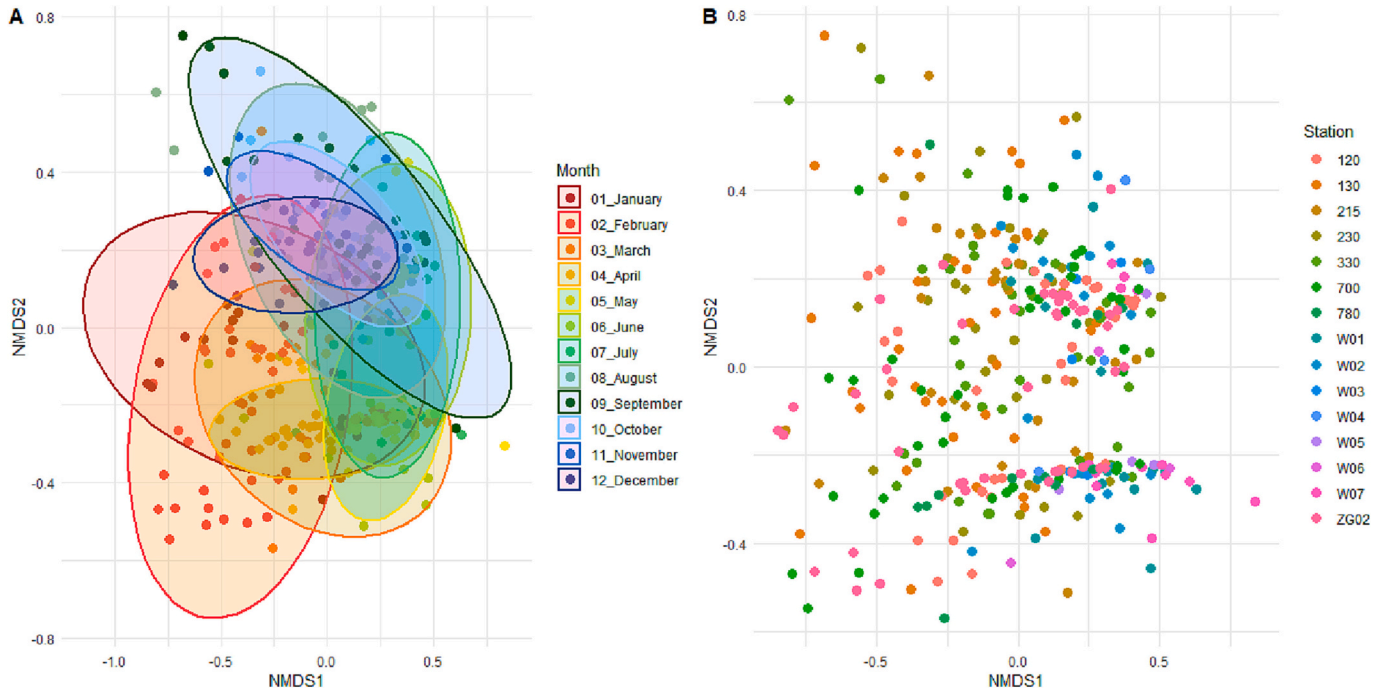

Fig. 5. Beta diversity (Bray–Curtis dissimilarity) ordinated with MDS of copepod communities. Each dot represents one individual plankton sample and each colour either constitutes either a sampling station or a sampling month, as depicted in the legend.

Table 1
Permutational multivariate analysis of variance (PERMANOVA) among the zooplankton communities of the different sampled stations and seasons. An asterisk denotes a statistically significant difference ($p < 0.01$).

	DF	SS	F. Model	R^2	P-value
Station	13	1.73	2.04	0.036	0.001*
Month	11	17.44	24.3	0.362	0.001*
Year	7	7.70	16.81	0.160	0.001*
Residuals	325	21.268	–	0.415	–
Total	356	48.142	–	1.00000	–

copepod species. Salinity is incorporated in the models of three copepod taxa (*T. longicornis, Centropages* spp. and *E. acutifrons*), while sum of PAH concentrations is included in three of the four models, yet only significant in one of the two *T. longicornis* models. Summed PCB concentrations were not significantly contributing to any model. Chlorophyll *a* concentrations were included in all models, but smooth terms were never significant.

The different variables have a different relative importance in explaining the observed variation in copepod abundances, and this was observed to be species-dependent (Fig. 8). Temperature, Secchi depth and chlorophyll concentrations consistently show high importance in the GAM models predicting the densities of the selected calanoid copepod taxa with relative contributions between 3.5 and 7.6 %. Temperature smoothers exhibit a conspicuous effect of the seawater temperature on the abundance of the different copepod species (Fig. 9, S10-S12). An optimal seawater temperature of 15–16 °C, alongside negative effects for higher water temperatures, can be found for *T. longicornis, Centropages* spp., and *A. clausi*. The shape of the effect of temperature on *A. clausi* is more complex compared to the other two species, with a temperature optimum found around 15 °C and a smaller second peak at approximately 7.5 °C (Fig. S10).

Salinity is a significant predictor, but negligible in terms of importance for the calanoid copepods *T. longicornis* (0.1 %) and *Centropages* spp. (1.8 %), and was not included in the *A. clausi* model. In contrast, *E. acutifrons* densities show a linear effect of salinity with positive effects at higher salinities (4.3 %), while this is the opposite for *T. longicornis and Centropages* densities (Fig. 9, S10, S12). *E. acutifrons* densities show a linear decreasing effect with increasing Secchi depth (less turbid), while exactly the opposite (and significant) trend visible for calanoid densities (Table 3, Fig. 9, S10-S12). Year is the only significant predictor for calanoid densities that was not included in the *E. acutifrons* model. Finally, the contribution of toxicant concentrations (summed PAH or PCB concentrations) is species-specific as well, with relative contributions of 0.1 and 3.3 %, but no significant trends for *E. acutifrons*.

4. Discussion

4.1. Spatiotemporal trends in the pelagic copepod community

Lengthy plankton data series allow to distinguish peculiar changes in species abundance and how they are affected by environmental changes such as climatic change (Kane and Prezioso, 2008). Our findings suggest that calanoid copepod abundances have significantly decreased compared to those reported 10 years ago. They reached an absolute minimum in 2018, and have been slowly recovering since then, only to collapse again in 2022 (Fig. 3). This decrease in abundance did not occur in densities of the harpacticoid *Euterpina,* as there were no significant increases or decreases of population abundances in the BPNS over time. Capuzzo et al. (2017) also reported decreasing abundance trends of the smaller copepods (four predominant taxa, i.e., *Temora*, *Acartia*, *Pseudocalanus* and *Paracalanus*) in the entire North Sea, using collated time-series from the Continuous Plankton Recorder (CPR) surveys that were run from 1988 to 2013. Moreover, the decreasing abundances of these copepods were accompanied by decreasing primary production, particularly at the transitional east region of the North Sea. Capuzzo et al. (2017) reported significant correlations among the observed changes in primary production and the higher trophic level dynamics, including (small) copepods and commercial fish stocks. However, the authors reported on a gradual decrease in the entire North Sea (including the Atlantic component), while, here we suggest a catastrophic effect of the heatwaves being at play in the nearshore/coastal part of the North Sea, ultimately also resulting in a decrease of the

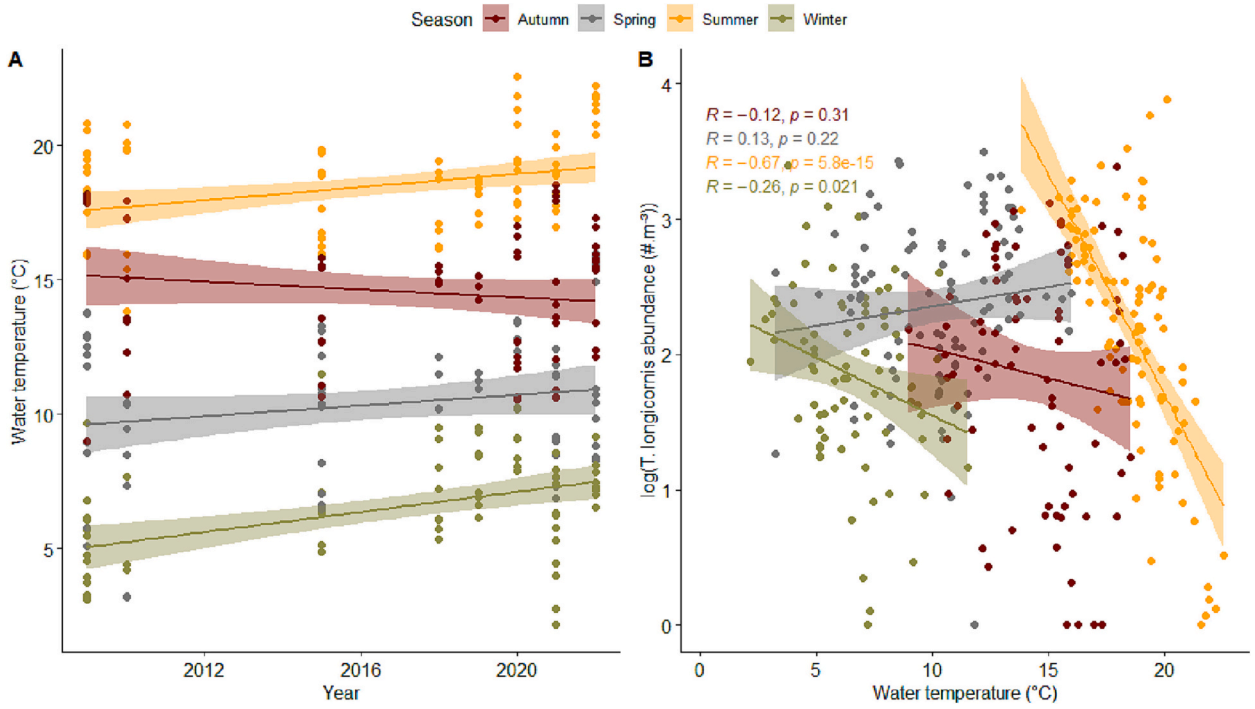

Fig. 6. (A) Trends in sea water temperature (°C) in the Belgian Part of the North Sea over the years, according to sampling season. (B) Relationship between log transformed *Temora longicornis* abundances and water temperatures. Shading shows the 95 % confidence level interval for model predictions. Spearman Rho values and *p*-values of the linear models are also shown. Relationship between water temperatures and other copepod abundances are visualised in Supplementary fig. S5.

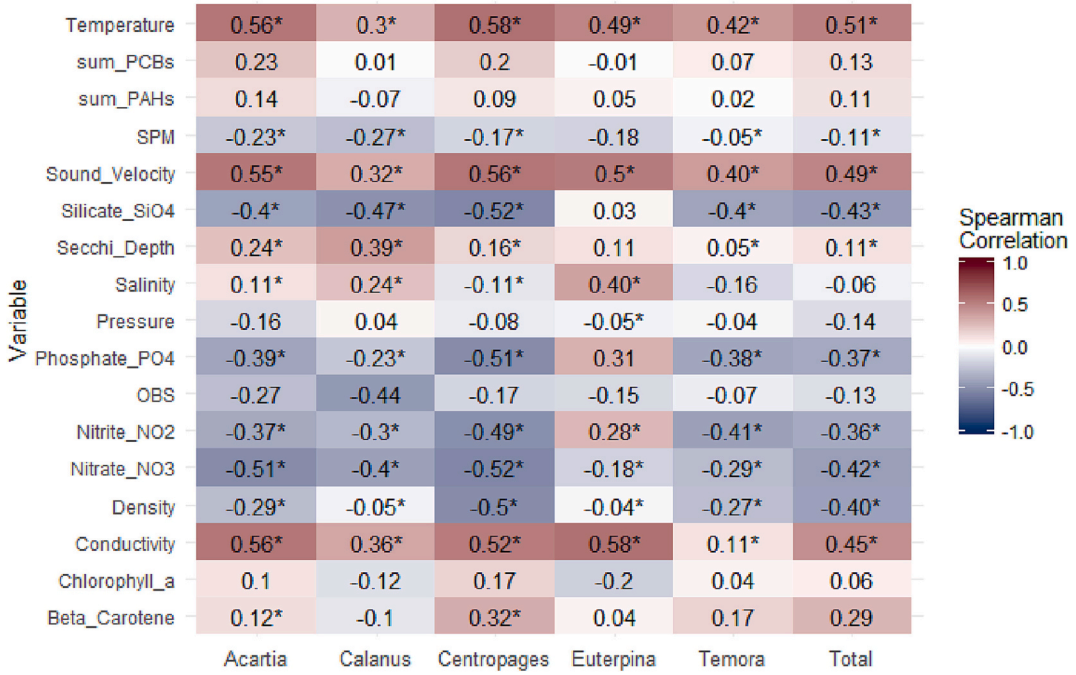

Fig. 7. Correlogram depicting the correlation (Spearman rank) between copepod densities (one column per species/taxon/sum) and measured environmental parameters (row). Spearman rho correlation coefficient is shown in each cell. Colour indicates the strength and direction of correlation, as depicted in the legend. Asterisks indicate significant correlations with a *p*-value smaller than 0.05.

copepod stocks. In contrast to our findings, Capuzzo et al. (2017) did not find significant decreases in the abundances of the larger copepod species (*Calanus* spp.) in the North Sea. Mortelmans et al. (2021), with their analysis at the copepod order level (Calanoida, Cyclopoida, Harpacticoida), also did not find any important changes in the average monthly abundances or total biomass estimates for the study period 2014–2020. This might be explained by a potential population size increase of other species that were not investigated in this study (e.g., *Paracalanus parvus*, *Pseudocalanus elongatus* or the recently invading *Pseudodiaptomus marinus*), compensating/replacing the losses in the population stocks of the studied taxa. Additionally, we have not investigated the dynamics of the naupliar stages of these species, as they are too small to be quantitatively

Table 2
The number of (official) heat waves affecting Belgium and the Belgian Part of the North Sea in the investigated time period. Start and end dates are reported, as well as the average maximal (daily) air temperature during the heatwave in Uccle and if possible at the buoy situated at the Thornton Bank (51.58 Lat., 2.993 Long.), approximately at 30 km off the Belgian coast (Sea Bruges). Additionally, maximal (daily) seawater temperatures at the beginning and the end of the heat wave are reported, the percentual change in temperature between these two values, as well as the average covering the entire heat wave. NA: written abbreviation for not applicable.

Start date	End date	Duration (days)	Average maximum air T in Uccle (°C)	Average maximum air T at buoy (°C)	Average maximum water T at buoy (°C)	Maximum water T at buoy (°C) at start of heat wave	Maximum water T at buoy (°C) at end of heat wave	% increase in water T
30 June 2015	05 July 2015	6	30.5	NA	NA	17.63	NA	NA
13 July 2018	27 July 2018	15	29.9	NA	20.66	19.46	21.35	9.7
29 July 2018	07 August 2018	10	30.1	NA	22.05	21.35	22.67	6.2
23 June 2019	30 June 2019	8	28.4	NA	NA	NA	NA	NA
22 July 2019	26 July 2019	5	33.8	NA	20.27	19.52	20.63	5.7
23 August 2019	28 August 2019	6	30.2	NA	19.97	20.05	19.85	−1.0
05 August 2020	16 August 2020	12	31.3	22.54	20.53	19.42	21.05	8.4
09 August 2022	16 August 2022	8	30.2	22.78	21.3	21.09	21.51	1.9

Table 3
GAM models relating the densities of *Temora longicornis, Acartia clausi, Centropages* spp. and *Euterpina acutifrons* to the environmental parameters. The environmental parameters that were chosen for the construction of the GAM models encompass water temperature (Temp), Secchi depth (Secchi), salinity (Sal), chlorophyll *a* concentrations (chl a) and summed PCB and/or PAH concentrations, respectively (sum_PAHs, sum_PCBs). Smooth terms with a significance <0.05 are denoted in bold. W_i = Akaike weight (Eq. 3), ER = evidence ratio (w_i best model/w_i model). Models most likely to be the best fitted model have an ER < 2.

	Model	Deviance explained (%)	AIC	W_i	ER
Temora longicornis	**Year** + **Temp** + Sal + **Secchi** + chl a + sum_PAHs + sum_PCBs	45.8	259.2034	0.42	1.39
	Year + **Temp** + **Secchi** + chl a + **sum_PAHs** + sum_PCBs	47.7	258.8726	0.58	1
Acartia clausi	**Year** + **Temp** + **Secchi** + chl a + **sum_PAHs** + sum_PCBs	58.9	204.3812	0.95	1
Centropages spp.	**Year** + **Temp** + **Sal** + **Secchi** + chl a + **sum_PAHs** + sum_PCBs	59.6	198.4973	0.76	1
Euterpina acutifrons	**Temp** + **Sal** + **Secchi** + chl a + sum_PCBs	49.6	337.6838	0.57	1

sampled with the 200 μm net used in the study. Outside the North Sea, in the offshore shelf waters of the Atlantic, Kane and Prezioso (2008) observed significant increases in *T. longicornis* abundance in the early 1990s until 2001, followed by a significant decline from 2002 till the remainder of the monitored time series (2006). Similarly, based on observations in the period 1958–2014 from the global ocean Continuous Plankton Recorder surveys in the North Atlantic and the Arctic, Edwards et al. (2016) reported more or less stable copepod abundances in offshore regions, while finding a decrease in abundance, particularly in the southern North Sea.

4.2. Impact of environmental variables on copepod abundance and distribution

In order to better understand the impact of the measured environmental factors and changes on the observed population trends, we applied generalized additive models to untangle the relative contribution of water temperature, turbidity, nutrient concentrations, salinity and persistent organic pollutants to the dynamics of these species in the BPNS. Importantly, in the current study, the generated GAM models did not consider any interactions between the abiotic variables and/or any biotic effects resulting from species interactions such as predation and competition. Similarly, other indirect effects, namely the impact on phytoplankton and protozooplankton (as food resources for copepods), the impact on microplankton (as a possible source of toxins and metabolites that might suppress copepod growth and development), the rapid increase of bacteria and viruses (as potential infection agents) have not been taken into account in the current study. We recognize these interactions should be taken into account when further interpreting the results, especially as we found significant correlations among the abundances of the studied calanoid species, but not with the harpacticoid species.

Temperature appears to be a key predictor for copepod abundance and diversity. This is in line with temperature being a major determinant for metabolic rates, body size, hatching success, development rate and/or fecundity of copepods (e.g., Devreker et al., 2005; Halsband-Lenk et al., 2002; Sahota et al., 2022), translating into the high relative importance that was found for this predictor for the abundances of the studied taxa (Fig. 8). The importance of temperature has also been reported as one of the main environmental drivers explaining zooplankton seasonality (e.g., in Fanjul et al., 2018a, 2018b). In general, the smoother predicted negative effects with increasing temperatures above 15–16 °C. The negative impact of higher sea water temperatures on calanoid copepods have already been reported in literature. For example, a zooplankton community analysis in Lake Baikal indicated significant increases in water temperature and corresponding subtle declines in copepod abundances (Hampton et al., 2008; Izmest'eva et al., 2016). Analysis of copepod time-series data from the eastern North Atlantic (Bay of Biscay and the Kattegat Sea) and the Mediterranean Sea (Gulf of Saronikos) revealed a high temporal turnover in the community composition and decreased similarity ('decay') over 3 decades (Villarino et al., 2020). According to the authors, these findings result from both environmental conditions and stochastic processes,

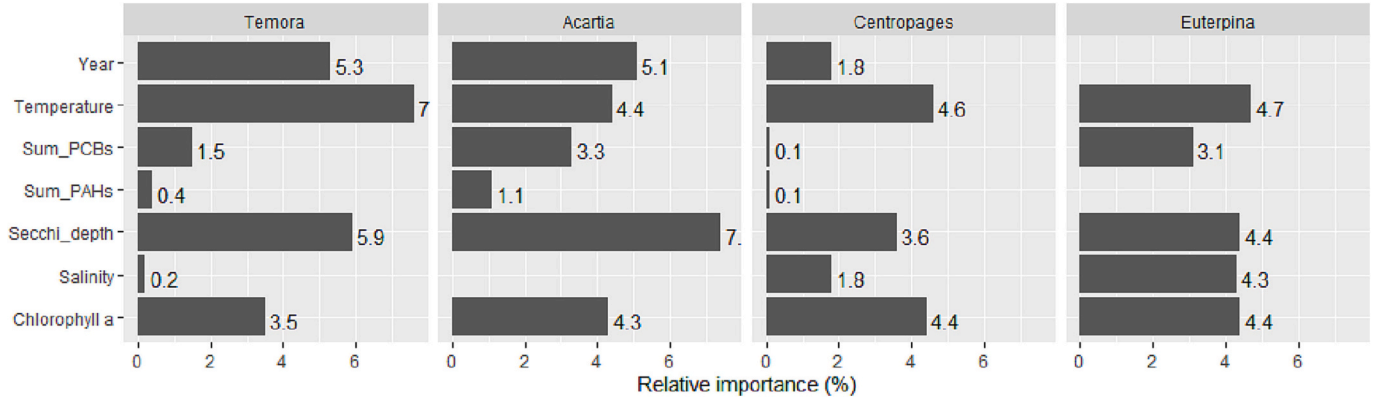

Fig. 8. Relative importance of the different parameters for the abundances of *Temora longicornis*, *Acartia clausi*, *Centropages* spp. and *Euterpina acutifrons* for the best fitted GAM model. Values of relative importance of each parameter are reported on the bar charts.

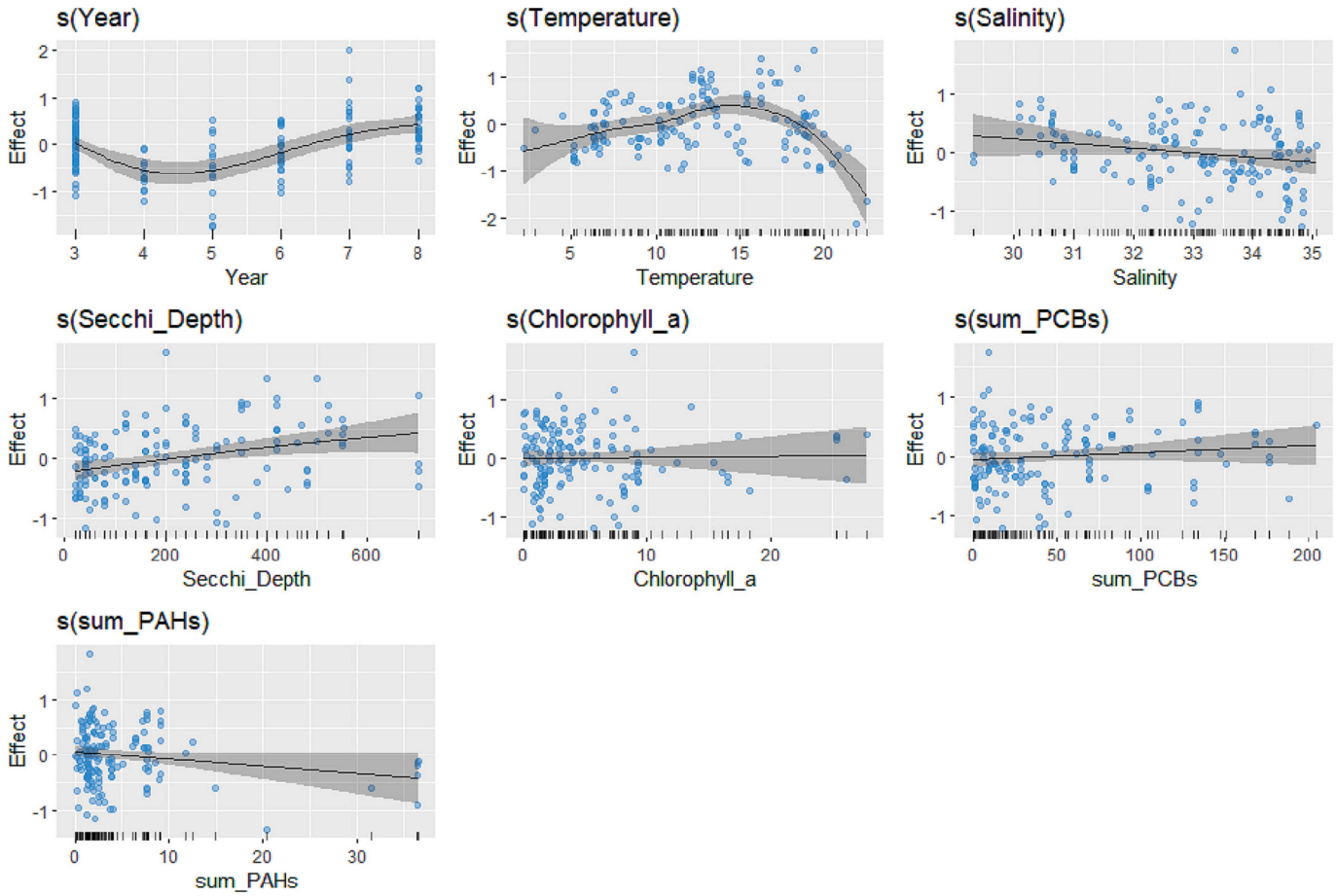

Fig. 9. Generalized additive model (GAM) plots showing the partial effects of selected explanatory variables on the log transformed abundances of *Temora longicornis* in the surveyed parts of the Belgian Part of the North Sea. The tick marks on the x-axis represent observed data points. The y-axis represents the partial effect of each variable. The shaded areas indicate the 95 % confidence intervals.

with stronger associations observed in areas experiencing higher ocean warming rates. Kane and Prezioso (2008) observed lower abundances of *T. longicornis* in the southern part of the US Northeast continental shelf in warmer and found sharp declines in the mean abundance as temperature rose in summer. *T. longicornis* abundance in the Middle Atlantic Bight was observed to be negatively correlated to surface temperature (Kane and Prezioso, 2008).

Surprisingly, we found negative correlations between phosphate and nitrate concentrations and calanoid copepod abundances (Fig. 7). This is most likely the result of changing phytoplankton conditions (changes in community composition and, by consequence, changes in the biochemical composition of the community as well), associated with fluctuations in the nutrient composition of the sea water. Future research should aim to associate these changes in the phytoplankton community with nutrient changes. Except for *Centropages* spp. and *A. clausi*, we did not find a significant positive correlation between copepod abundance and chlorophyll *a* or β carotene concentrations. However, the smoothers for chlorophyll *a* concentrations were not

significant in the GAM models and could not predict decreases in densities with increasing chlorophyll *a* levels.

Except for *A. clausi*, salinity contributed significantly to copepod dynamics, albeit of low importance (Fig. 8; cf. the findings of Deschutter et al., 2017). This is most likely due to the facts that salinities in general were generally stable and stayed within the preferred range for these species. The smoothers predict in general a decrease in densities with increasing salinity for the calanoid copepods, while the smoothers predict exactly the opposite for *E. acutifrons*. Based on the 2015 dataset, Deschutter et al. (2017) found a similar trend for the calanoid copepods. In contrast, Kane and Prezioso (2008) found through correlation analysis that the interannual variability of *T. longicornis* densities showed a significant negative relationship with surface salinity anomalies in the southern part of the US Northeast continental shelf.

Finally, our study aimed at confirming whether mixtures of PCB and PAH concentrations significantly contributed to the copepod's densities. We did not find significant correlations between summed PCB/PAH concentrations and population size. Except for *E. acutifrons*, both summed PCB and PAH concentrations were included in the best GAM model, yet only the sum_PAH smoother contributed significantly in predicting densities. The models suggest a decrease in copepod abundances with increasing concentrations of the PAH mixture present in the BPNS. Yet, the left part of the smoother for the summed PAH concentrations accommodates the majority of the data points and displays decreased copepod abundances up to intermediate toxicant concentrations (except for *A. clausi*). The right section of the smoother is based on far fewer data points, so we have to be cautious to interpret this smoother, as we should emphasize on the zone holding most of the data. As more 'extreme' data points can steer the shape of the smoother, the effects of the mixed toxicants on copepods should be studied in a laboratory context with a dedicated experiment. Nevertheless, both in the current dataset and the dataset collected by Deschutter et al. (2017) the quantified PAH concentrations stayed below the EQS thresholds (Table S3), while PCB concentrations often exceeded the EQS values in both studies. Based on our results, there was no significant impact of exposure to these PCB concentrations to any studied copepod species. Applying GAMs to this dataset increased our comprehension on the effects of multiple drivers on the plankton community and the pelagic ecosystem, and, hence, might encourage the facilitation of future risk characterisation of chemicals, as it will allow a prioritisation of monitoring needs in terms of pollution. However, it is important to note that based on these results, we cannot exclude out potential effects of other toxicants in the BPNS.

4.3. Climate change impacting copepod populations through marine heat waves

This is, as far as we know, the first study to describe the impact of temperature increases on copepod populations in shallow, coastal areas, the North Sea or the Atlantic Ocean in general. Significantly higher summer surface temperatures were observed to coincide with a collapse in the populations of the dominant calanoid copepod species, i.e., *T. longicornis*, *Centropages* spp. and *A. clausi*. During the summers of 2018, 2019, 2020 and 2022 heat waves were recorded in this region, resulting in exceptionally warm seawater temperatures (Table 2). For example, temperatures in August 2020 and 2022 in the more nearshore situated stations reached 22–22.5 °C during the sampling campaign. Also, more offshore, at the Thorntonbank, a maximum temperature of 22.67 °C was recorded during a MHW event (July 2018; Table 2). These temperature values are close to/already exceeding the thermal tolerance limits of the calanoid species investigated (Table 4). In the case of *T. longicornis*, this means that the water temperatures have already reached the thermal physiological threshold of 22.5 °C (Halsband-Lenk et al., 2002), coinciding with a collapse of the populations at these locations (e.g., with resulting densities as low as 0.57–2.25 ind.m^{-3} in August 2020, or 0–0.55 ind. m^{-3} in August 2022, whereas August densities in the period 2009–2015 reached on average at least 226 ind. m^{-3}, with a minimum of 26.25 ind.m^{-3}; Table S1). Despite decreasing temperatures in the succeeding months, densities remained low or absent, probably as the populations require more time to recover, causing an absence of the typical autumn peak for this species (e.g., in 2018, 2022; Fig. 2). For example, in September 2022, *T. longicornis* was still completely absent in all collected zooplankton samples, although the seawater temperature had by then dropped to a non-critical 17.3 °C (station 330). This recovery period extended to December 2022, impacting the observed (negative) correlation between water temperature and *T. longicornis* densities in winter (Fig. 6B). Excluding the 2022 event, this correlation is no longer significant.

Table 4
Thermal tolerance for the studies copepod species, obtained from literature.

Species	Observation	Reference
Acartia clausi	Upper lethal temperature between 27 and 34 °C (depending on acclimatization period)	González, 1974
Calanus helgolandicus	Thermal niche ranging from 3 to 22 °C	Bonnet et al., 2008
Centropages hamatus	Upper thermal limit 25 °C (female); thermal tolerance range between 2 and 25 °C	Halsband-Lenk et al., 2002
Centropages typicus	Upper thermal limit 30 °C (female); thermal tolerance range between 2 and 30 °C	Halsband-Lenk et al., 2002
Euterpina acutifrons	Upper thermal limit of 31 °C; Optimal growth rate between 25 and 27 °C	Amatus et al., 2020
Temora longicornis	Upper thermal limit 22.5 °C (female); thermal tolerance range between 0 and 22.5 °C	Halsband-Lenk et al., 2002
	Significant decrease in survival rate (22.5 ± 14.7 %) after exposure to 23 °C for 6 days; rapid depletion of fatty acid content	Sahota et al., 2022

These observations are relevant in the global change framework, as sea water temperatures are expected to continue to rise (Bindoff et al., 2007; Levitus et al., 2000). Using the Institut Pierre Simon Laplace (IPSL) Earth System Model, Chust et al. (2014) estimated that, by the end of this century, an increase in ocean temperature of 2.29 ± 0.05 °C will cause global phytoplankton and zooplankton biomass to decrease by 6 % and 11 %, respectively. Their results indicate that both globally, as well as in the Atlantic Margin and the North Sea, an elevated ocean stratification will cause primary production and, consequently, zooplankton biomass to decrease in regards to a warming climate, whereas primary production and zooplankton biomass will expand in both the Barents and Baltic Sea (Chust et al., 2014). However, concurrent with the long-term persistent warming of our oceans and seas, discrete periods of extreme regional ocean warming (termed marine heatwaves, MHWs) have grown in frequency (Coumou and Rahmstorf, 2012; Perkins et al., 2012). Projections indicate these MHWs will occur more frequently, intensively and for longer periods throughout the twenty-first century (Meehl and Tebaldi, 2004). In Belgium, since 1900, 46 heatwaves have been registered, of which 16 have occurred since the year 2000 (RMI, 2022). Marine heat waves are known to potentially impact marine ecosystems and their services, by causing a redistribution of marine biogeography, with anomalous appearances/absences of species outside of their known geographical range (McKinstry et al., 2022; Suryan et al., 2021). The deleterious impacts of prominent heatwaves across a range of biological processes and taxa, mainly corals, seagrasses and kelps (Smale et al., 2019), have been reported, but the impact of MHWs on zooplankton has been understudied. In the Gulf of Alaska (Pacific Ocean), Batten et al. (2022) did observe a few rare taxa from the zooplankton community being absent during a MHW event in 2015–2016, while no common taxa disappeared from the community (although some fluctuations in relative abundance were observed).

Our results demonstrate that the pelagic copepod community in the North Sea is affected by significant warming of the sea water, to which heatwave events are contributing. Not only directly affecting the copepod's physiology, copepod predators such as the dinoflagellate *Noctiluca scintillans,* as well as cnidarians and ctenophores, are known to be

favored by warmer seawater temperatures, which both can significantly impact copepod populations, as discussed in Wright et al. (2021) and Mortelmans et al. (2021). Blooms of these gelatinous taxa have already been recorded at several occasions in the BPNS in 2018, 2019 and 2020 (Ollevier et al., 2021). So far, we do not know the additional impact of these events on the copepod community in the BPNS. Finally, it will also be important to study how these changes in the zooplankton community are affecting other trophic levels in the benthopelagic food web, such as phytoplankton and pelagic fish stocks. As has been shown by Van Ginderdeuren et al. (2013), the pelagic fish stocks in the BPNS, tend to select for a few, larger copepod species, such as *T. longicornis*, regardless of abundance of prey item. How will pelagic fish populations react to shifts in zooplankton composition and availability? Beaugrand et al. (2003) have already described how the virtual absence of *C. finmarchicus* due to rising water temperatures (and its replacement by the smaller *C. helgolandicus*) resulted in a lower copepod biomass leading to an all-time low in cod recruitment in the North Sea (bottom-up control). Regardless, this study is a valuable first step in improving our apprehension of the impact of warming and MHW events on the entire pelagic community in the North Sea and its consequences for the carbon sink.

5. Conclusion

Our study provides evidence that climate change related and other anthropogenic processes are altering North Sea ecosystems today. The studied time series revealed a significant decrease (up to 2-fold) in four of the dominant zooplankton species in the BPNS, i.e., the calanoid copepods *Temora longicornis*, *Acartia clausi*, *Centropages* spp., and *Calanus helgolandicus*. Temperature was one of the predictors consistently manifesting a major importance in all GAM models predicting the densities of the selected copepod taxa, while summed PAH or PCB concentrations were not able to explain the observed spatiotemporal trends. The several heat waves during the summer months of the monitored years, and the resulting increased water temperatures, are most likely the cause for the calanoid copepod declines, as they corresponded to the physiological thermal limit of some of the studied species. In essence, our study emphasizes the importance of long-term time series in key oceanographic characteristics, including zooplankton abundances, as they are known to ultimately affect other components of the pelagic and benthic ecosystems.

Authors' contributions

All the authors contributing to this work are listed in the names section. Ilias Semmouri and Colin Janssen designed and conceptualized the study with input from all co-authors. Ilias Semmouri wrote the main manuscript text. Ilias Semmouri and Jonas Mortelmans contributed in data collection and analysis. Ilias Semmouri, Karel De Schamphelaere, Colin Janssen, Jan Mees and Jana Asselman discussed and interpreted the results critically. Jana Asselman, Colin Janssen, Jan Mees provided funding. All authors reviewed the manuscript.

Declaration of competing interest

The authors declare that they have no known competing financial interests or personal relationships that could have appeared to influence the work reported in this paper.

Data availability

Data will be made available on request.

Acknowledgements

We are thankful to the Flanders Marine Institute (VLIZ) and the LifeWatch project, a Flemish contribution to the LifeWatch ESFRI by VLIZ, for their financial and technical support, a special thanks to the crew of the research vessel Simon Stevin. We thank Yana Deschutter, Marleen De Troch, Jolien Depecker and Nancy De Saeyer for the technical assistance. The research leading to the data presented in this publication was carried out with infrastructure partially funded by LifeWatch ESFRI and EMBRC Belgium – FWO project GOH3817N.

Appendix A. Supplementary data

Supplementary data to this article can be found online at https://doi.org/10.1016/j.marpolbul.2023.115159.

References

Amatus, M., Basri, N.A., Shapawi, R., Muhamad Shaleh, S.R., 2020. Effect of temperature on population growth of copepod, *Euterpina acutifrons*. Borneo Journal of Marine Science and Aquaculture (BJoMSA) 4 (1), 57–61. https://doi.org/10.51200/bjomsa.v4i1.2620.

Anderson, M.J., 2001. A new method for non-parametric multivariate analysis of variance: non-parametric manova for ecology. Austral Ecol. 26, 32–46. https://doi.org/10.1111/j.1442-9993.2001.01070.pp.x.

Batten, S., Clark, R., Flinkman, J., Hays, G., John, E., John, A.W., Jonas, T., Lindley, J.A., 2003. CPR sampling: the technical background, materials and methods, consistency and comparability. Prog. Oceanogr. 58, 193–215. https://doi.org/10.1016/j.pocean.2003.08.004.

Batten, S.D., Ostle, C., Hélaouët, P., Walne, A.W., 2022. Responses of gulf of Alaska plankton communities to a marine heat wave. Deep-Sea Res. II Top. Stud. Oceanogr. 195, 105002 https://doi.org/10.1016/j.dsr2.2021.105002.

Beaugrand, G., Brander, K.M., Alistair Lindley, J., Souissi, S., Reid, P.C., 2003. Plankton effect on cod recruitment in the North Sea. Nature 426, 661–664. https://doi.org/10.1038/nature02164.

Bellier, E., Engen, S., Jensen, T.C., 2022. Seasonal diversity dynamics of a boreal zooplankton community under climate impact. Oecologia 199, 139–152.

Bindoff, N.L., Willebrand, J., Artale, V., Cazenave, A., Gregory, J., Gulev, S., Hanawa, K., Solomon, S., Qin, D., Manning, M., Chen, Z., Marquis, M., Averyt, K.B., Tignor, M., et al., 2007. Observations: Oceanic climate change and sea level, climate change 2007: The physical science basis. In: Contribution of Working Group I to the Fourth Assessment Report of the Intergovernmental Panel on Climate Change. Cambridge University Press, Cambridge.

Bonnet, D., Harris, R.P., Yebra, L., Guilhaumon, F., Conway, D.V., Hirst, A.G., 2008. Temperature effects on *Calanus helgolandicus* (copepoda: Calanoida) development time and egg production. J. Plankton Res. 31 (1), 31–44. https://doi.org/10.1093/plankt/fbn099.

Burnham, K.P., Anderson, D.R., 2003. Model Selection and Multimodel Inference: A Practical Information-Theoretic Approach. Springer Science & Business Media.

Buttay, L., Miranda, A., Casas, G., González-quirós, R., Nogueira, E., 2015. Long-term and seasonal zooplankton dynamics in the northwest Iberian shelf and its relationship with meteo-climatic and hydrographic variability. J. Plankton Res. 38 (1), 106–121. https://doi.org/10.1093/plankt/fbv100.

Capuzzo, E., Lynam, C., Barry, J., Stephens, D., Forster, R., Greenwood, N., et al., 2017. A decline in primary production in the North Sea over 25 years, associated with reductions in zooplankton abundance and fish stock recruitment. Glob. Chang. Biol. 24 (1), e352–e364. https://doi.org/10.1111/gcb.13916.

Castellani, C., Edwards, M., 2017. Marine Plankton: A Practical Guide to Ecology, Methodology, and Taxonomy. Oxford University Press, Oxford, UK, p. 704.

Cavanaugh, J., Neath, A., 2019. The Akaike information criterion: background, derivation, properties, application, interpretation, and refinements. Wires Comput. Stat. 11 (3) https://doi.org/10.1002/wics.1460.

Chen, W., Staneva, J., Grayek, S., Schulz-Stellenfleth, J., & Greinert, J. (2022). The role of heat wave events in the occurrence and persistence of thermal stratification in the southern North Sea. Nat. Hazards Earth Syst. Sci., 22(5), 1683–1698. doi:https://doi.org/10.5194/nhess-22-1683-2022.

Cheng, L., Abraham, J., Hausfather, Z., Trenberth, K.E., 2019. How fast are the oceans warming? Science 363 (6423), 128–129. https://doi.org/10.1126/science.aav7619.

Chiou, C.T., 1985. Partition coefficients of organic compounds in lipid-water systems and correlations with fish bioconcentration factors. Environ. Sci. Technol. 19 (1), 57–62.

Chust, G., Allen, J., Bopp, L., Schrum, C., Holt, J., Tsiaras, K., et al., 2014. Biomass changes and trophic amplification of plankton in a warmer ocean. Glob. Chang. Biol. 20 (7), 2124–2139. https://doi.org/10.1111/gcb.12562.

Coumou, D., Rahmstorf, S., 2012. A decade of weather extremes. Nat. Clim. Chang. 2 (7), 491–496. https://doi.org/10.1038/nclimate1452.

Cumming, H., Rücker, C., 2017. Octanol–water partition coefficient measurement by a simple 1H NMR method. ACS Omega 2 (9), 6244–6249. https://doi.org/10.1021/acsomega.7b01102.

Daro, M.H., Breton, E., Antajan, E., Gasparini, S., Rousseau, V., 2006. Do *Phaeocystis* colony blooms affect zooplankton in the Belgian coastal zone? In: Rousseau, V., et al. (Eds.), Current Status of Eutrophication in the Belgian Coastal Zone, pp. 61–72.

Deschutter, Y., Everaert, G., De Schamphelaere, K.A.C., De Troch, M., 2017. Relative contribution of multiple stressors on copepod density and diversity dynamics in the Belgian part of the North Sea. Mar. Pollut. Bull. 125 (1–2), 350–359. https://doi.org/10.1016/j.marpolbul.2017.09.038.

Devreker, D., Souissi, S., Seuront, L., 2005. Effects of chlorophyll concentration and temperature variation on the reproduction and survival of *Temora longicornis* (Copepoda, Calanoida) in the eastern English Channel. J. Exp. Mar. Biol. Ecol. 318 (2), 145–162. https://doi.org/10.1016/j.jembe.2004.12.011.

ECHA, 2008. Guidance on information requirements and chemical safety assessment. Chapter R. 8.

Edwards, M., Helaouet, P., Alhaija, R.A., Batten, S., Beaugrand, G., Chiba, S., et al., 2016. *Global Marine Ecological Status Report: Results from the Global CPR Survey 2014/2015*. SAHFOS Technical Report No. 11. SAHFOS, Plymouth.

Fanjul, A., Iriarte, A., Villate, F., Uriarte, I., Artiach, M., Atkinson, A., Cook, K., 2018a. Latitude, distance offshore and local environmental features as modulators of zooplankton assemblages across the NE Atlantic Shelves Province. J. Plankton Res. 41 (3), 293–308. https://doi.org/10.1093/plankt/fbz015.

Fanjul, A., Iriarte, A., Villate, F., Uriarte, I., Atkinson, A., Cook, K., 2018b. Zooplankton seasonality across a latitudinal gradient in the Northeast Atlantic shelves province. Cont. Shelf Res. 160, 49–62. https://doi.org/10.1016/j.csr.2018.03.009.

Flanders Marine Institute (VLIZ), Belgium (2021): LifeWatch observatory data: monthly CTD temperature and salinity measurements in the Belgian Part of the North Sea. https://rshiny.lifewatch.be/ctd-data/.

Flanders Marine Institute (2022): ICOS and LifeWatch observatory data: buoy data doi: 10.14284/536. Accessed through the LifeWatch Data Explorer / lwdataexplorer R package.

Flanders Marine Institute (VLIZ), Belgium (2021b): LifeWatch observatory data: nutrient, pigment, suspended matter and Secchi measurements in the Belgian Part of the North Sea. doi:10.14284/441.

González, J.G., 1974. Critical thermal maxima and upper lethal temperatures for the calanoid copepods *Acartia tonsa* and *A. clausi*. Mar. Biol. 27, 219–223. https://doi.org/10.1007/BF00391947.

Gorsky, G., Grosjean, P., 2003. Qualitative and quantitative assessment of zooplankton samples. GLOBEC International Newsletter 9, 5.

Grosjean, P., Picheral, M., Warembourg, C., Gorsky, G., 2004. Enumeration, measurement, and identification of net zooplankton samples using the ZOOSCAN digital imaging system. ICES J. Mar. Sci. 61 (4), 518–525. https://doi.org/10.1016/j.icesjms.2004.03.012.

Halsband-Lenk, C., Hirche, H., Carlotti, F., 2002. Temperature impact on reproduction and development of congener copepod populations. J. Exp. Mar. Biol. Ecol. 271 (2), 121–153. https://doi.org/10.1016/s0022-0981(02)00025-4.

Hampton, S.E., Izmest'eva, L.R., Moore, M.V., Katz, S.L., Dennis, B., Silow, E.A., 2008. Sixty years of environmental change in the world's largest freshwater Lake - Lake Baikal, Siberia. Glob Change Biol. 14, 1947–1958. https://doi.org/10.1111/j.1365-2486. 2008.01616.x.

Hays, G., Richardson, A., Robinson, C., 2005. Climate change and marine plankton. Trends Ecol. Evol. 20 (6), 337–344. https://doi.org/10.1016/j.tree.2005.03.004.

He, S., 2004. Generalized additive models for data with Concurvity: statistical issues and a novel model fitting approach. University of Pittsburgh. 1–51.

Hobday, A.J., Alexander, L.V., Perkins, S.E., Smale, D.A., Straub, S.C., Oliver, E.C., Wernberg, T., 2016. A hierarchical approach to defining marine heatwaves. Prog. Oceanogr. 141, 227–238. https://doi.org/10.1016/j.pocean.2015.12.014.

Hobday, A., Oliver, E., Sen Gupta, A., Benthuysen, J., Burrows, M., Donat, M., Smale, D., 2018. Categorizing and naming marine heatwaves. Oceanography 31 (2). https://doi.org/10.5670/oceanog.2018.205.

Holmlund, C.M., Hammer, M., 1999. Ecosystem services generated by fish populations. Ecol. Econ. 29, 253–268. https://doi.org/10.1016/S0921-8009(99)00015-4.

IPCC, 2019. In: Pörtner, H.-O., Roberts, D.C., Masson-Delmotte, V., Zhai, P., Tignor, M., Poloczanska, E., Mintenbeck, K., Alegría, A., Nicolai, M., Okem, A., Petzold, J., Rama, B., Weyer, N.M. (Eds.), IPCC Special Report on the Ocean and Cryosphere in a Changing Climate. Cambridge University Press, Cambridge, UK and New York, NY, USA. https://doi.org/10.1017/9781009157964, 755p.

IPCC, 2021. In: Masson-Delmotte, V., Zhai, P., Pirani, A., Connors, S.L., Péan, C., Berger, S., Caud, N., Chen, Y., Goldfarb, L., Gomis, M.I., Huang, M., Leitzell, K., Lonnoy, E., Matthews, J.B.R., Maycock, T.K., Waterfield, T., Yelekçi, O., Yu, R., Zhou, B. (Eds.), Climate Change 2021: The Physical Science Basis. Contribution of Working Group I to the Sixth Assessment Report of the Intergovernmental Panel on Climate Change. Cambridge University Press, Cambridge, United Kingdom and New York, NY, USA. https://doi.org/10.1017/9781009157896, 2391 pp.

Izmest'eva, L.R., Moore, M.V., Hampton, S.E., Ferwerda, C.J., Gray, D.K., Woo, K.H., Pislegina, H.L., Krashchuk, L.S., Shimaraeva, S.V., Silow, E.A., 2016. Lake-wide physical and biological trends associated with warming in Lake Baikal. J. Great Lakes Res. 42, 6–17. https://doi.org/10.1016/j.jglr.2015.11.006.

Kane, J., Prezioso, J., 2008. Distribution and multi-annual abundance trends of the copepod *Temora longicornis* in the US northeast shelf ecosystem. J. Plankton Res. 30 (5), 619–632. https://doi.org/10.1093/plankt/fbn026.

Kessler, A., Goris, N., Lauvset, S.K., 2022. Observation-Based Sea surface temperature trends in Atlantic large marine ecosystems. Prog. Oceanogr. 208, 102902 https://doi.org/10.1016/j.pocean.2022.102902.

Kiørboe, T., 2001. Formation and fate of marine snow: small-scale processes with large-scale implications. Sci. Mar. 65, 57–71. https://doi.org/10.3989/scimar.2001.65s257.

Lacroix, G., Ruddick, K., Ozer, J., Lancelot, C., 2004. Modelling the impact of the Scheldt and Rhine/Meuse plumes on the salinity distribution in Belgian waters (southern North Sea). J. Sea Res. 52 (3), 149–163. https://doi.org/10.1016/j.seares.2004.01.003.

Lescrauwaet, A.-K., Pirlet, H., Verleye, T., Mees, J., & Herman, R., (2013). Compendium voor Kust en Zee 2013: Een geïntegreerd kennisdocument over de socio-economische, ecologische en institutionele aspecten van de kust en zee in Vlaanderen en België. Vlaams Instituut voor de Zee (VLIZ): Oostende. ISBN 978-90-820731-5-7. 342 pp.

Levitus, S., Antonov, J.I., Boyer, T.P., Stephens, C., 2000. Warming of the world ocean. Science 287, 2225–2229. https://doi.org/10.1126/science.287.5461.2225.

McCarty, L.S., Mackay, D., 1993. Enhancing ecotoxicological modeling and assessment. Body residues and modes of toxic action. Environ. Sci. Technol. 27 (9), 1718–1728.

McKinstry, C.A.E., Campbell, R.W., Holderied, K., 2022. Influence of the 2014–2016 marine heatwave on seasonal zooplankton community structure and abundance in the lower Cook inlet, Alaska. Deep-Sea Res. II Top. Stud. Oceanogr. 195, 105012 https://doi.org/10.1016/j.dsr2.2021.105012.

Meehl, G.A., Tebaldi, C., 2004. More intense, more frequent, and longer lasting heat waves in the 21st century. Science 305 (5686), 994–997. https://doi.org/10.1126/science.1098704.

Mortelmans, J., Goossens, J., Amadei Martínez, L., Deneudt, K., Cattrijsse, A., Hernandez, F., 2019. LifeWatch observatory data: zooplankton observations in the Belgian part of the North Sea. Geoscience Data Journal 6 (2), 76–84. https://doi.org/10.1002/gdj3.68.

Mortelmans, J., Aubert, A., Reubens, J., Otero, V., Deneudt, K., Mees, J., 2021. Copepods (Crustacea: Copepoda) in the Belgian part of the North Sea: trends, dynamics and anomalies. J. Mar. Syst. 220, 103558 https://doi.org/10.1016/j.jmarsys.2021.103558.

O'Brien, T.D., Wiebe, P.H., Hay, S.J., 2011. ICES Zooplankton Status Report 2008/2009, Cooperative Research Report No. 307. International Council for the Exploration of the Sea, Copenhagen, Denmark.

O'Brien, T.D., Lorenzoni, L., Isensee, K., Valdes, L., 2017. What are marine ecological time series telling us about the ocean? A status report. IOC Tech. Ser. 129, 1–297.

Oksanen, J., Blanchet, F.G., Kindt, R., Legendre, P., Minchin, P.R., O'Hara, R.B., Simpson, G.L., Solymos, P., Stevens, M.H.H. and Wagner, H. (2015). Vegan: community ecology package. R Package Version 2.2-0. Retrieved August 21, 2020 from http://CRAN.Rproject.org/package=vegan.

Ollevier, A., Mortelmans, J., Aubert, A., Deneudt, K., Vandegehuchte, M., 2021. *Noctiluca scintillans*: dynamics, size measurements and relationships with small soft-bodied plankton in the Belgian part of the North Sea. Front. Mar. Sci. 8 https://doi.org/10.3389/fmars.2021.777999.

Perkins, S.E., Alexander, L.V., Nairn, J.R., 2012. Increasing frequency, intensity and duration of observed global heatwaves and warm spells. Geophys. Res. Lett. 39 (20) https://doi.org/10.1029/2012gl053361.

RMI, 2022. Retrieved 21 November 2022, from. https://www.meteo.be/nl/klimaat/klimaatverandering-in-belgie/klimaattrends-in-ukkel/luchttemperatuur/zomer-indices/hittegolven/hittegolven-in-ukkel.

Sahota, R., Boyen, J., Semmouri, I., Bodé, S., De Troch, M., 2022. An inter-order comparison of copepod fatty acid composition and biosynthesis in response to a long-chain PUFA deficient diet along a temperature gradient. Mar. Biol. 169 (10) https://doi.org/10.1007/s00227-022-04121-z.

Semmouri, I., De Schamphelaere, K.A.C., Mees, J., Janssen, C.R., Asselman, J., 2020a. Evaluating the potential of direct RNA nanopore sequencing: Metatranscriptomics highlights possible seasonal differences in a marine pelagic crustacean zooplankton community. Mar. Environ. Res. 153, 104836 https://doi.org/10.1016/j.marenvres.2019.104836.

Semmouri, I., De Schamphelaere, K.A.C., Van Nieuwerburgh, F., Deforce, D., Janssen, C. R., Asselman, J., 2020b. Spatio-temporal patterns in the gene expression of the calanoid copepod *Temora longicornis* in the Belgian part of the North Sea. Mar. Environ. Res. 160, 105037 https://doi.org/10.1016/j.marenvres.2020.105037.

Semmouri, I., De Schamphelaere, K.A.C., Willemse, S., Vandegehuchte, M., Janssen, C.R., Asselman, J., 2021. Metabarcoding reveals hidden species and improves identification of marine zooplankton communities in the North Sea. ICES J. Mar. Sci. fsaa256 https://doi.org/10.1093/icesjms/fsaa256.

Smale, D.A., Wernberg, T., Oliver, E.C., Thomsen, M., Harvey, B.P., Straub, S.C., Moore, P.J., 2019. Marine heatwaves threaten global biodiversity and the provision of ecosystem services. Nat. Clim. Chang. 9 (4), 306–312. https://doi.org/10.1038/s41558-019-0412-1.

Climate change 2013: Working group 1 (WG1). In: Stocker, T., Dahe, Q., Plattner, G.-K., et al. (Eds.), 2013. Contribution to the Intergovernmental Panel on Climate Change (IPCC) 5th Assessment Report (AR5). Cambridge University Press.

Suryan, R.M., Arimitsu, M.L., Coletti, H.A., Hopcroft, R.R., Lindeberg, M.R., Barbeaux, S. J., Batten, S.D., Burt, W.J., Bishop, M.A., Bodkin, J.L., Brenner, R., Campbell, R.W., Cushing, D.A., Danielson, S.L., Dorn, M.W., Drummond, B., Esler, D., Gelatt, T., Hanselman, D.H., Zador, S.G., 2021. Ecosystem response persists after a prolonged marine heatwave. Sci. Rep. 11 (1) https://doi.org/10.1038/s41598-021-83818-5.

Symonds, M.R., Moussalli, A., 2011. A brief guide to model selection, multimodel inference and model averaging in behavioural ecology using Akaike's information criterion. Behav. Ecol. Sociobiol. 65 (1), 13–21. https://doi.org/10.1007/s00265-010-1037-6.

Townsend, M., Davies, K., Hanley, N., Hewitt, J., Lundquist, C., Lohrer, A., 2018. The challenge of implementing the marine ecosystem service concept. Front. Mar. Sci. 5 https://doi.org/10.3389/fmars.2018.00359.

Van Ginderdeuren, K., Vandendriessche, S., Prössler, Y., Matola, H., Vincx, M., Hostens, K., 2013. Selective feeding by pelagic fish in the Belgian part of the North Sea. ICES J. Mar. Sci. 71 (4), 808–820. https://doi.org/10.1093/icesjms/fst183.

Van Ginderdeuren, K., Van Hoey, G., Vincx, M., Hostens, K., 2014. The mesozooplankton community of the Belgian shelf (North Sea). J. Sea Res. 85, 48–58.

Villarino, E., Irigoien, X., Villate, F., Iriarte, A., Uriarte, I., Zervoudaki, S., Carstensen, J., O'Brien, T., Chust, G., 2020. Response of copepod communities to ocean warming in three time-series across the North Atlantic and Mediterranean Sea. Mar. Ecol. Prog. Ser. 636, 47–61. https://doi.org/10.3354/meps13209.

Vlaamse regering (2010). 21 MEI 2010. — Besluit van de Vlaamse Regering tot wijziging van het besluit van de Vlaamse Regering van 6 februari 1991 houdende vaststelling van het Vlaams reglement betreffende de milieuvergunning en van het besluit van de Vlaamse Regering van 1 juni 1995 houdende algemene en sectorale bepalingen inzake milieuhygiëne, voor wat betreft de milieukwaliteitsnormen voor oppervlaktewateren, waterbodems en Groundwater. Belgisch staatsblad. (09.07.10).

Wexels Riser, C., Wassmann, P., Olli, K., Pasternak, A., Arashkevich, E., 2002. Seasonal variation in production, retention and export of zooplankton faecal pellets in the marginal ice zone and the Central Barents Sea. J. Mar. Syst. 38, 175–188.

Williams, R., Conway, D.V.P., Hunt, H.G., 1994. The role of copepods in the planktonic ecosystem of mixed and stratified waters of the European shelf seas. Hydrobiologia 292-293 (1), 521–530.

Wood, S., 2006. Generalized Additive Models: An Introduction with R. Chapman & Hall/CRC, Boca Raton, US (391 pp.).

Wood, S., 2010. Fast stable restricted maximum likelihood and marginal likelihood estimation of semiparametric generalized linear models. Journal Of The Royal Statistical Society: Series B (Statistical Methodology) 73 (1), 3–36. https://doi.org/10.1111/j.1467-9868.2010.00749.x.

Wood, S., & Wood, M.S. (2016). Package 'mgcv'. R Package Version. pp. 1–7.

Wright, R.M., Le Quéré, C., Buitenhuis, E., Pitois, S., Gibbons, M.J., 2021. Role of jellyfish in the plankton ecosystem revealed using a global ocean biogeochemical model. Biogeosciences 18 (4), 1291–1320. https://doi.org/10.5194/bg-18-1291-2021.

Zuur, A.F., Ieno, E.N., Walker, N.J., Saveliev, A.A., Smith, G.M., 2009. Mixed effects models and extensions in ecology with R. In: Public Health, vol. 36. Springer, New York.